Recent developments in delta wing aerodynamics

I. Gursul
Department of Mechanical Engineering
University of Bath
Bath, UK

ABSTRACT

Recent developments in delta wing aerodynamics are reviewed. For slender delta wings, recent investigations shed more light on the unsteady aspects of shear-layer structure, vortex core, breakdown and its instabilities. For nonslender delta wings, substantial differences in the structure of vortical flow and breakdown may exist. Vortex interactions are generic to both slender and nonslender wings. Various unsteady flow phenomena may cause buffeting of wings and fins, however, vortex breakdown, vortex shedding, and shear layer reattachment are the most dominant sources. Dynamic response of vortex breakdown over delta wings in unsteady flows can be characterised by large time lags and hysteresis, whose physical mechanisms need further studies. Unusual flow–structure interactions for nonslender wings in the form of self-excited roll oscillations have been observed. Recent experiments showed that substantial lift enhancement is possible on a flexible delta wing.

NOMENCLATURE

AR	amplitude ratio; aspect ratio
b	span
c	root chord length
C_L	lift coefficient
C_μ	momentum coefficient
f	frequency
k	reduced frequency; axial wave number
n	wave number in angular direction
p	pressure fluctuation
r	correlation coefficient
R	amplitude of free stream variation
Re	Reynolds number based on chord length
s	local semispan
St	Strouhal number
t	time; thickness of delta wing
T	period
u	axial velocity
U_∞	free stream velocity
U_{jet}	jet velocity
v	swirl velocity
x	chordwise distance
x_{bd}	breakdown location
y	spanwise distance
y_f	fin location
z	vertical distance above wing surface
α	angle-of-attack
ϕ	roll angle; incidence of measurement plane
Γ	circulation
Λ	sweep angle
ν	kinematic viscosity
τ	time constant
ω	vorticity; radial frequency

1.0 INTRODUCTION

Delta wings are used in a variety of aerospace vehicles. Highly swept wings have many advantages in highly manoeuvrable fighter aircraft and supersonic civil transport. Current and future unmanned combat air vehicles are similar to delta wings with low sweep angles. Vortical flows are also dominant for mini- and micro-air vehicles operating in the low Reynolds number regime.

Many investigations have been carried out on the aerodynamics of slender delta wings. The flow over a slender delta wing at high angles-of-attack is dominated by two large, counter-rotating leading-edge vortices that are formed by the roll-up of vortex sheets as sketched in Fig. 1. The flow separates from the leading edge of the wing to form a curved free shear layer above the suction side of the wing, which rolls up into a core. The development of the leading-edge vortex, generation of large axial and swirl velocity components and resulting low pressure in the vortex core, which generate additional suction and lift force on the delta wings, have been studied in

Paper No. 2894. Manuscript received 29 April 2004, accepted 6 July 2004.
The latest in an occasional series of survey papers by leaders in their field.

https://doi.org/10.1017/S0001924000000269 Published online by Cambridge University Press

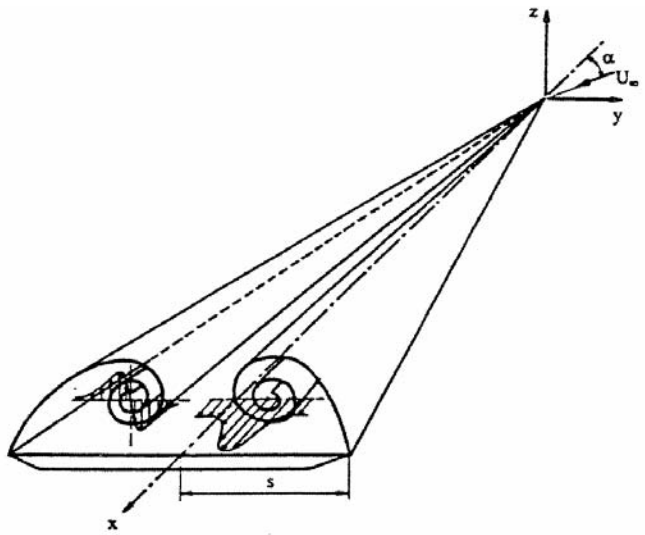


Figure 1. Schematic of shear layer and leading-edge vortices over a delta wing.

detail by previous investigators as summarised by Lee and Ho[1].

At a sufficiently high angle-of-attack, the vortices undergo a sudden expansion known as vortex breakdown, which was first observed by Werle[2] in 1954 in a water tunnel facility. A great deal of effort has been focused on the study of these vortices, vortex breakdown phenomenon, and aerodynamics of delta wings, as summarised in several review articles[1, 3].

There has been less emphasis on the unsteady aspects of these flows, which have an impact on aircraft stability and control, and wing/fin buffeting. Unsteady flow structure and aspects of the vortex breakdown phenomenon have been reviewed by Rockwell[4] and Visbal[5]. A wide range of unsteady phenomena relevant to vortex flows over stationary and manoeuvring slender delta wings has been reviewed by Gursul[6].

All these reviews point out that, for slender wings, there remain many aspects of vortical flows and delta-wing aerodynamics that are little understood. Recent investigations have shed more light on the structure of vortices and the breakdown process. As the historical focus has been on slender wings, there is very little known about nonslender delta wings. Recent work shows that both slender and nonslender wings have generic features, such as vortex–vortex interactions. The characteristics of wing and fin buffeting depend on the wing sweep angle. With the requirement for high manoeuvrability and increasing wing flexibility for future unmanned air vehicles, unsteady vortex flows and vortex–structure interactions are becoming more predominant. The objective of this article is to review the recent developments in delta wing aerodynamics, and to summarise the remaining issues and challenges. Although past achievements will be briefly mentioned, the emphasis is on new developments and the identification of areas that require further study, rather than presenting a broad review of the area.

2.0 SLENDER DELTA WINGS

2.1 Leading-edge vortices

In this review article, slender wings are defined as those with sweep angles equal to or larger than 65 degrees ($\Lambda \geq 65^{\circ}$). Leading-edge vortices over slender wings develop very strong axial flows in the core as the separated shear layers roll-up. The time-averaged axial velocity is roughly axisymmetric and its maximum can be as large as four or five times the free stream velocity.

The separated shear layers sketched in Fig. 1 roll up periodically

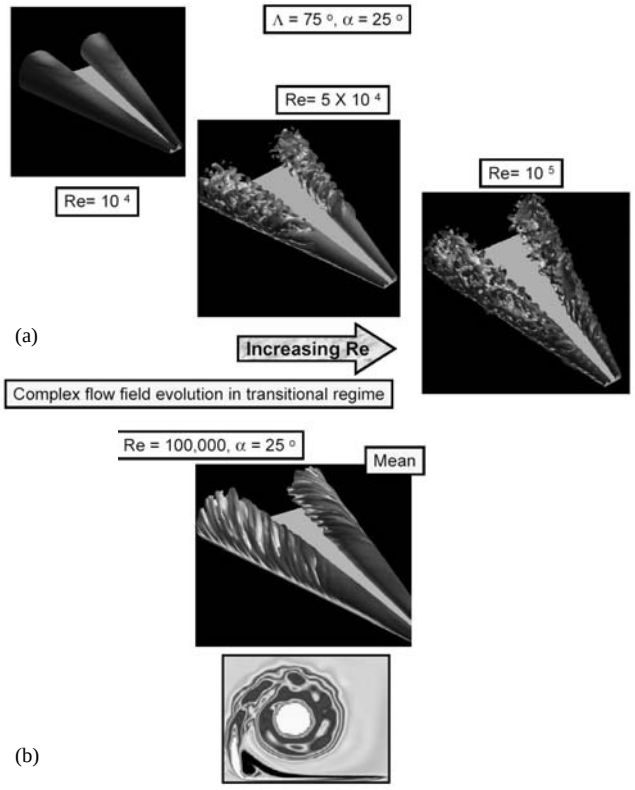


Figure 2. (a) Instantaneous flow showing the transition process with increasing Reynolds number; (b) time-averaged flow showing mean vortical substructures[14].

into discrete vortical substructures, as visualised by Gad-el-Hak and Blackwelder[7] over a delta wing. This phenomenon was attributed to a Kelvin-Helmholtz type instability of the shear layer. The unsteady Kelvin-Helmholtz (K-H) instability was observed by flow visualisation[7], hot-wire velocity measurements[8], particle image velocimetry measurements[9, 10] and numerical simulations[11]. In both experiments[9] and computations[11], the observed frequencies were found to be in agreement with the predictions from the linear stability analysis of the cross-flow shear layer. Therefore, the unsteady K-H instability over delta wings is a generic part of the flow as much as it is for two-dimensional shear layers.

On the other hand, several researchers[12, 13] have revealed the existence of stationary, small-scale vortices around the primary vortex, as opposed to those that rotate around the primary vortex. The origin of these steady structures is not well understood and has been subject to a variety of hypotheses. The spatially fixed substructures were measured by velocity probes at fixed locations, and were identified as a result of time-averaging the flow. Their relation to the temporal substructures was recently demonstrated by direct numerical simulations[14]. Instantaneous flow shows the temporal substructures and the transition process with increasing Reynolds number (see Fig. 2). More interestingly, the time-averaged flow shows isosurfaces of the time-averaged axial vorticity and mean vortical substructures. These results indicate that ‘steady’ and ‘unsteady’ substructures are not necessarily two separate phenomena. Details of shear layer structure and transition need to be investigated further.

Even at low incidences long before vortex breakdown appears over the wing, leading-edge vortices exhibit highly unsteady flow. It was shown by Menke and Gursul[15] that large amplitude velocity fluctuations occur in the absence of breakdown over delta wings. The variation of rms swirl velocity is sketched in Fig. 3. The rms swirl velocity is large within the subcore and reaches its maximum at the axis of the time-averaged vortex. The maximum rms swirl velocity can exceed the free stream velocity depending on the angle-of-attack. These large

https://doi.org/10.1017/S0001924000000269 Published online by Cambridge University Press

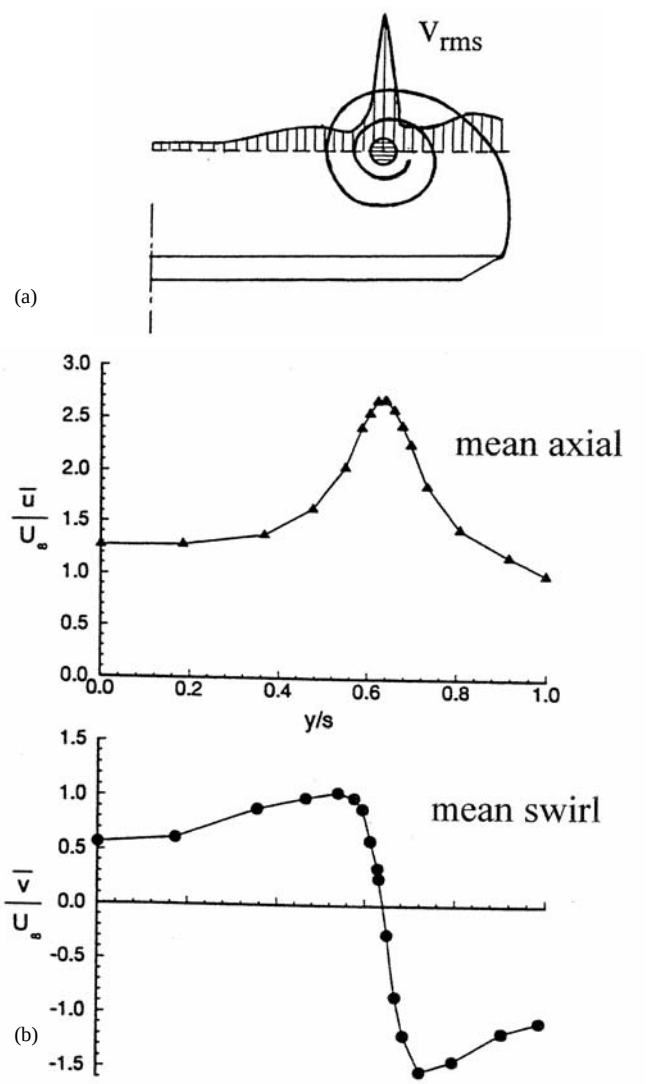


Figure 3. (a) Variation of rms swirl velocity across the vortex core; (b) time-averaged axial and swirl velocity profiles[15].

amplitude, broad band velocity fluctuations, which are observed in a variety of vortex flows[6], are due to random displacements of the vortex core. This 'wandering' of the vortex core has also been observed in tip vortices trailing from rectangular wings[16, 17].

Several possibilities for the origin of vortex wandering have been suggested. For example, it is suggested in the investigations by Baker *et al*[16] and Devenport *et al*[17] that vortex wandering in tip vortices is due to free stream turbulence. Several possibilities, including the Kelvin-Helmholtz instability in the shear layer and the unsteady turbulent wake of the wing, were discussed as potential sources of vortex wandering over delta wings[15]. The role of the shear layer instabilities was later clarified by comparing velocity fluctuations in the core in the absence and presence of the Kelvin-Helmholtz instability[18]. A definite correlation between vortex wandering and the presence of the Kelvin-Helmholtz instability was demonstrated. This is explained by the Biot-Savart induction of small-scale vortices, which displace the primary vortex. Nonlinear interactions of small vortices and the primary vortex lead to random displacements of the primary vortex core. Further studies are needed for better understanding of vortex wandering, which is important for the development of the vortex core properties.

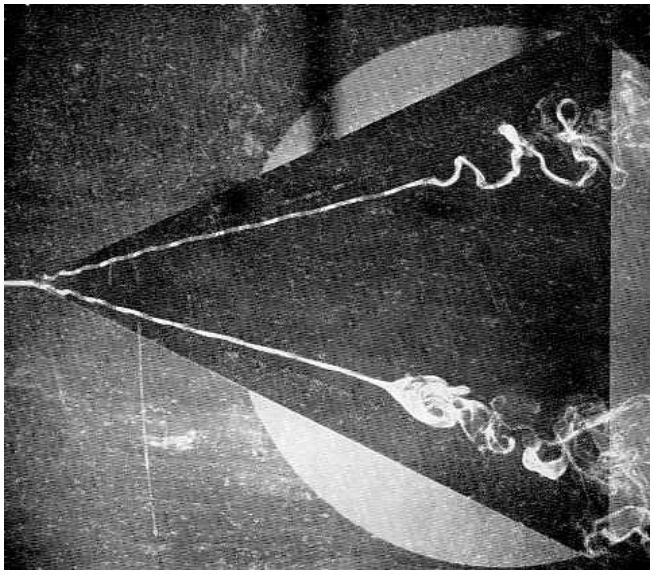


Figure 4: Flow visualisation of vortex breakdown over a delta wing[19].

2.2 Vortex breakdown

Vortex breakdown is an intriguing phenomenon that has been observed on delta wings. Vortex breakdown has adverse effects on the time-averaged performance for slender wings. For example, the magnitude of the lift and pitching moment decreases after vortex breakdown. Flow visualisation conducted by Lambourne and Bryer[19] revealing the so-called 'bubble' type and 'spiral' type vortex breakdowns is shown in Fig. 4. Subsequent research suggested that the spiral type is more common over delta wings. In fact, even the bubble type of vortex breakdown switches to the spiral type from time to time in experiments. Different explanations of the vortex breakdown phenomenon based on hydrodynamic instability, wave propagation, and flow stagnation are summarised in several review articles[20-22]. It is now generally agreed that this phenomenon is a wave propagation phenomenon, and there is a strong analogy to shocks in gas dynamics. Both experiments and theoretical explanations show that there are two important parameters affecting the occurrence and movement of vortex breakdown: swirl level and external pressure

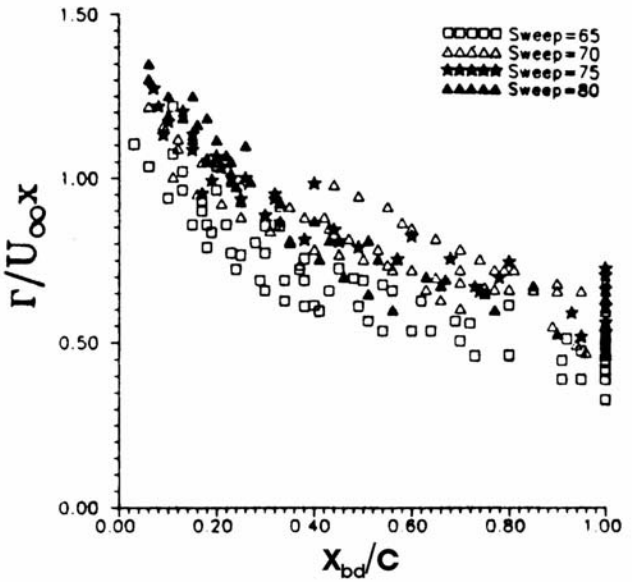


Figure 5. Scatter of vortex breakdown location in different facilities[23]. Source of data for each sweep angle are given in Ref. 23.

https://doi.org/10.1017/S0001924000000269 Published online by Cambridge University Press

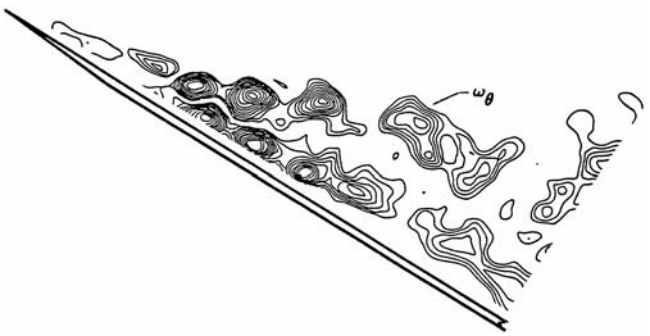


Figure 6. Intantaneous azimuthal vorticity distribution in a plane that passes through the axis[27].

gradient outside the vortex core. An increase in either parameter promotes the earlier occurrence of breakdown. For leading-edge vortices, both parameters depend on the wing geometry, such as incidence and sweep angle.

Experimental investigations show that large scatter appears in the vortex breakdown location (see Fig. 5, taken from Gursul[23]). Geometric variations of wing, tunnel wall effects, support interference, model deformations, Reynolds number (believed to have negligible effect for slender wings, but more important for nonslender wings), unsteady nature of breakdown location, and measurement methods are all possible sources of the large scatter. Figure 5 also shows the sensitivity of the vortex breakdown phenomenon to the geometric parameters which alter the external pressure gradient for the vortical flow. Hall[21] has shown that small external pressure gradients can be amplified along the core of the vortices, leading to a stagnation point. Thus, the large sensitivity of the breakdown location to a streamwise pressure gradient along the exterior of the vortex is very much expected.

It is well known that the flow downstream of vortex breakdown exhibits a well-documented flow instability. Periodic oscillations have been observed in a variety of swirling flows after breakdown occurred. When vortex breakdown moves over the wing[24], the amplitude of the quasi-periodic pressure fluctuations increases. Experimentally observed periodic velocity/pressure oscillations[24-26] correspond to the most unstable normal modes of the time-averaged velocity profiles of the vortex (downstream of breakdown) based on the linearised, inviscid stability analysis. The disturbances are represented as $\exp\{i(kx + n\phi - \omega t)\}$, where ω is the frequency, k the wave number in the axial direction, and n the wave number in the angular direction. By using two-point pressure measurements in the axial and spanwise directions[25], it was demonstrated that these fluctuations are due to the first helical mode ($n = 1$). Experiments also indicate that the frequency decreases in the streamwise direction, which implies that the pitch of the helix increases in the streamwise direction. This was confirmed by the instantaneous azimuthal vorticity distribution[27] in a plane that passes through the axis (see Fig. 6). The vorticity concentrations are staggered like a Karman vortex street and the spacing increases in the streamwise direction.

Also, this description of the helical mode instability is consistent with well-known observations of the spiral breakdown over delta wings. It is well known that this is the dominant mode observed over delta wings. Analysing flow visualisation studies in wind tunnels, Jumper *et al*[28] indicated that even in the cases where breakdown looked like a bubble type, a spiral form was identified in instantaneous pictures with a short exposure time. This supports the view that the spiral form is a consequence of the instability of the bubble form. For spiral breakdown, the sense of the helix is opposite to the direction of rotation in the main vortex as observed over delta wings.

The pitch (wavelength) of the helical mode instability increases in the streamwise direction, while the frequency decreases. Measurements of pressure fluctuations at different streamwise locations on delta wings suggest that the dimensionless frequency fx/U_∞ is nearly

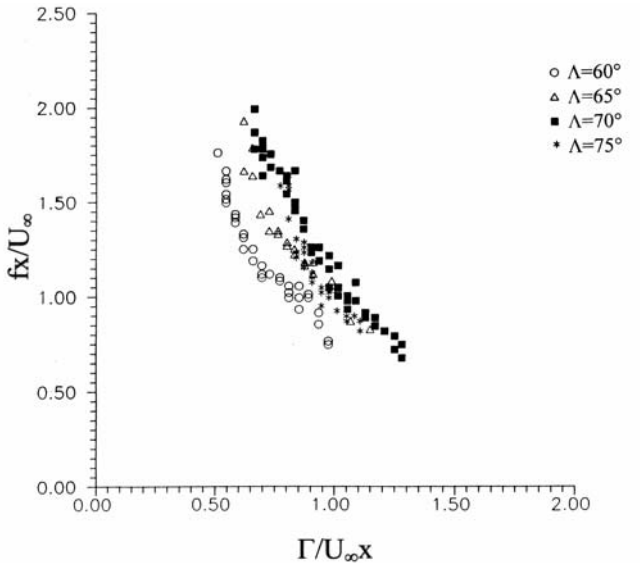


Figure 7. Variation of dimensionless frequency as a function of dimensionless circulation[25].

constant for a given geometry[25]. Knowledge of the dominant frequency of the helical mode instability as a function of wing geometry (angle-of-attack and sweep angle) is important for buffeting problems, particularly fin buffeting. Gursul[25] suggested that the dimensionless frequency fx/U_∞ is a function of $\Gamma/U_\infty x$, where Γ is the circulation of the leading-edge vortex, as shown in Fig. 7 for wings with different sweep angles. Note that the dimensionless number $\Gamma/U_\infty x$ is related to the rate of increase of the circulation along the streamwise direction (or the rate at which vorticity is fed into the leading-edge vortex) for a conical flow. It should be noted that these data are valid for vortex breakdown naturally occurring over slender delta wings. However, at smaller angles-of-attack, breakdown can be induced, for example, by the presence of a fin. There are no available data on the dominant frequencies for this type of premature vortex breakdown, which would be useful for fin-buffeting predictions.

3.0 NONSLENDER DELTA WINGS

Aerodynamics of nonslender wings exhibits distinct differences. For example, lift force continues to increase even after vortex breakdown is present over the wing[29, 30]. The vortical flow over nonslender delta wings ($\Lambda \leq 55°$) also has major differences. The vortices form much closer to the surface of the wing[31], and vortex–boundary layer interaction becomes important at low Reynolds numbers[32, 33]. It was found that there is a profound effect of Reynolds number on the structure of vortical flows. The images in Fig. 8 show the vortices generated over the wing at an incidence of $\alpha = 5°$ for three different Reynolds numbers. Vortex breakdown of leading-edge vortices at the trailing edge of the wing is visible for Re = 8,700. A further increase in Reynolds number resulted in the upstream progression of the breakdown of the vortices, which is a curious result considering the accepted insensitivity of vortices and vortex breakdown over more slender wings. When the Reynolds number is nearly tripled to Re = 26,000, the vortex breakdown location moves to nearly 40% of the chord length. In general, the breakdown of the leading-edge vortices is delayed significantly, and the vortices form more inboard at low Reynolds numbers. Experiments[33] suggest that there is very little change in the structure of vortices and location of breakdown for Re ≥ 25,000 for a sweep angle of $\Lambda = 50°$.

Also apparent in Fig. 8 was the formation of an additional vortex outboard of the primary vortex, which indicated the existence of a dual vortex structure. It was shown[34] that the secondary vortex

https://doi.org/10.1017/S0001924000000269 Published online by Cambridge University Press

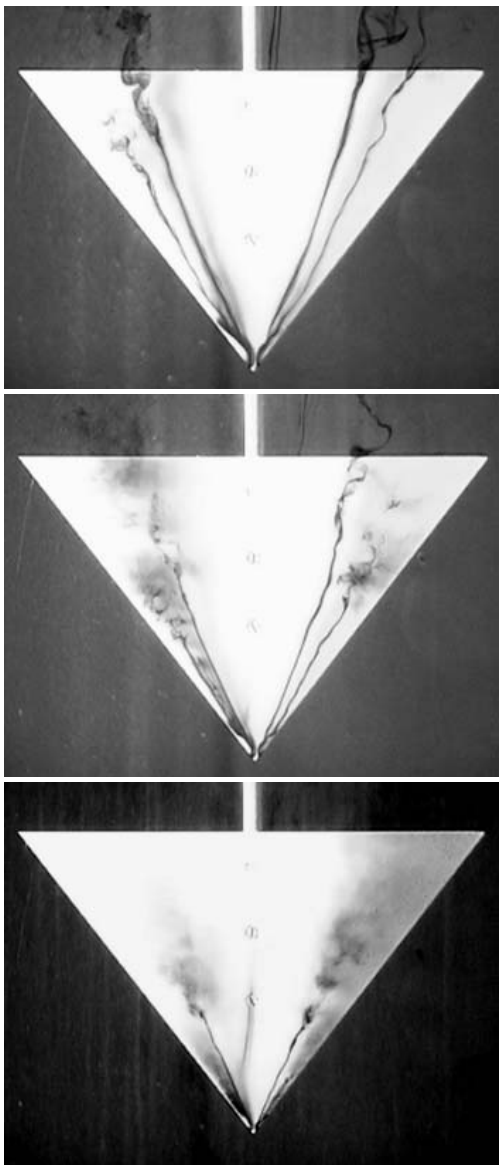


Figure 8. Dye flow visualisation of vortex flows for $\alpha = 5°$, $\Lambda = 50°$, (Ref. 33).

effectively splits the primary vortex into two separate concentrations of vorticity, resulting in a dual vortex structure at small incidences (see Fig. 9). It is noted that this structure is strongly affected by the Reynolds number. A single layer of vorticity concentration was observed at very low Reynolds numbers (on the order of a few thousands) and the dual vortex structure was absent. With increasing Reynolds number, the significant interaction between the boundary layer and primary vortex results in this dual-vortex structure. The images presented in Fig. 8 indicate that the outboard pair of vortices undergoes breakdown further upstream than the primary (inboard) pair in all the cases considered herein. This dual vortex structure diminishes and a single primary vortex is observed at higher incidences.

Even at low angles-of-attack, such as a few degrees, there are vortical flows and vortex breakdown[33]. In Fig. 10, dye flow visualisation is shown at small incidences. The interesting feature was the occurrence of breakdown over the wing at $\alpha = 2{\cdot}5°$. At such a low incidence one would not normally expect to observe breakdown, especially so far forward on the wing. In Fig. 10, surface flow visualisation is also shown for a much higher Reynolds number. The surface flow patterns clearly show the existence of the primary reattachment and secondary separation lines even at low incidences, indicating the presence of strong vortical flows over the lifting surface. The reattachment line is visible all the way to the trailing edge for small incidences, but only the initial part of it near the apex is easy to identify with increasing incidence. The reattachment line moves towards the centreline of the wing with increasing incidence. The secondary separation line reveals a change in curvature at around 30 to 40% of

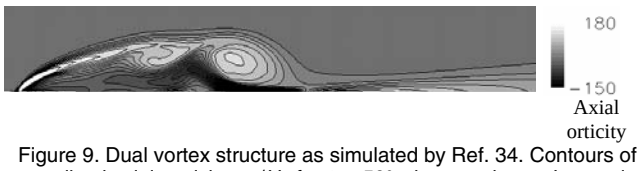


Figure 9. Dual vortex structure as simulated by Ref. 34. Contours of normalised axial vorticity $\omega c/U_\infty$ for $\Lambda = 50°$ wing are shown. Interaction with boundary-layer vorticity results in primary vortex being split into two vortices.

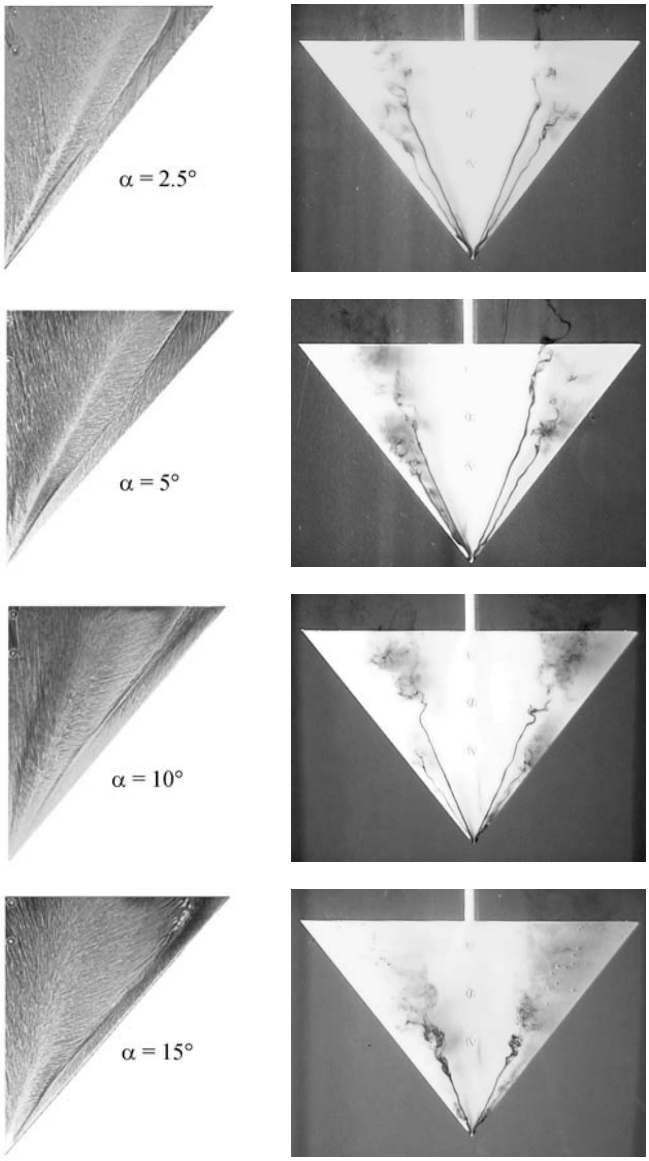


Figure 10. (a) Surface flow visualisation at Re = 10^6; (b) flow visualisation pictures of vortex breakdown for varying incidence, Re = 13,000, $\Lambda = 50°$ (Ref. 35).

https://doi.org/10.1017/S0001924000000269 Published online by Cambridge University Press

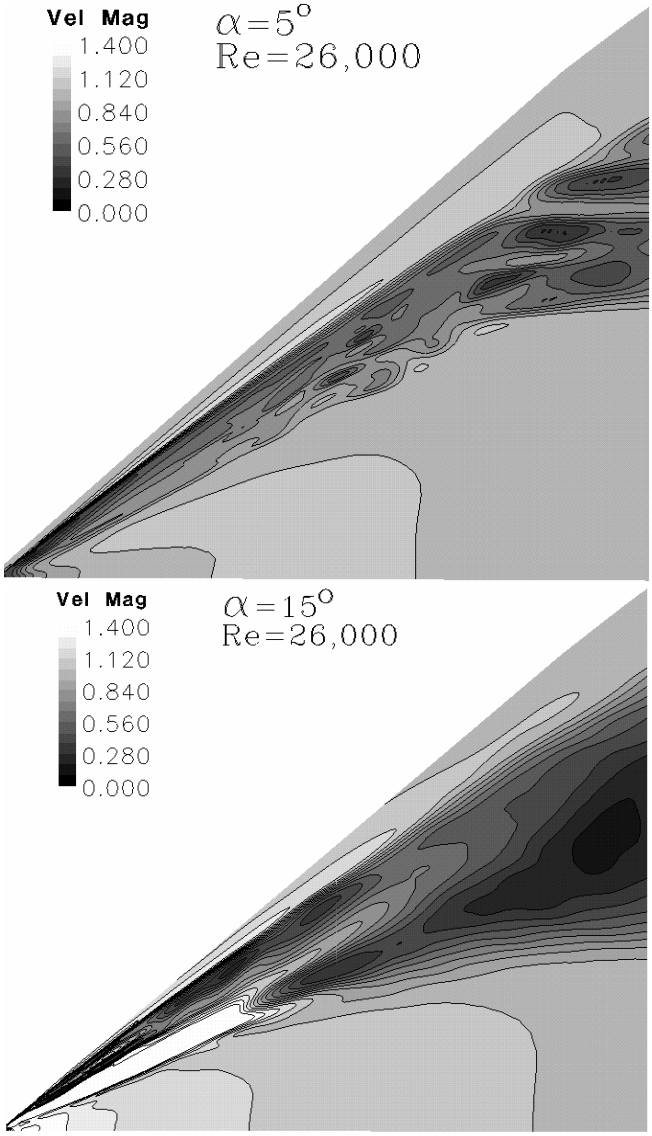


Figure 11. Magnitude of time-averaged velocity in a plane through the vortex core[34]. Velocity is normalised with free stream velocity.

the chord length from the apex for $\alpha \leq 15^{\circ}$. This is most likely to be a consequence of vortex breakdown for this nonslender wing rather than the transition of the boundary layer as discussed in Ref. 29.

Vortex breakdown may be very different for nonslender wings. Gordnier and Visbal[34] showed that vortex breakdown is very difficult to identify based on the time-averaged velocity field at low incidences (for example, $\alpha = 5^{\circ}$ in Fig. 11). In general, vortex breakdown is much milder compared to that of slender wings, and the deceleration of the axial velocity is much smaller. Also, typical high axial velocities upstream of breakdown for slender wings are not observed at low incidences. A jet-like axial velocity is only observed at higher incidences (see $\alpha = 15^{\circ}$ in Fig. 11), and the vortex breakdown resembles that of slender wings.

Figure 12 shows the magnitude of the time-averaged velocity in a plane through the vortex core in the PIV experiments[35]. For $\alpha = 10^{\circ}$, there is no indication of vortex breakdown, although flow visualisation revealed the bubble-like breakdown at a time-averaged location of $x/c \approx 0{\cdot}40$. Hence both upstream and downstream of breakdown there exists wake-like axial flow. Very low velocity regions are visible for $x/c \geq 0{\cdot}7$, but there is again no evidence of a breakdown based on velocity magnitude shown in Fig. 12. In general, at small incidences,

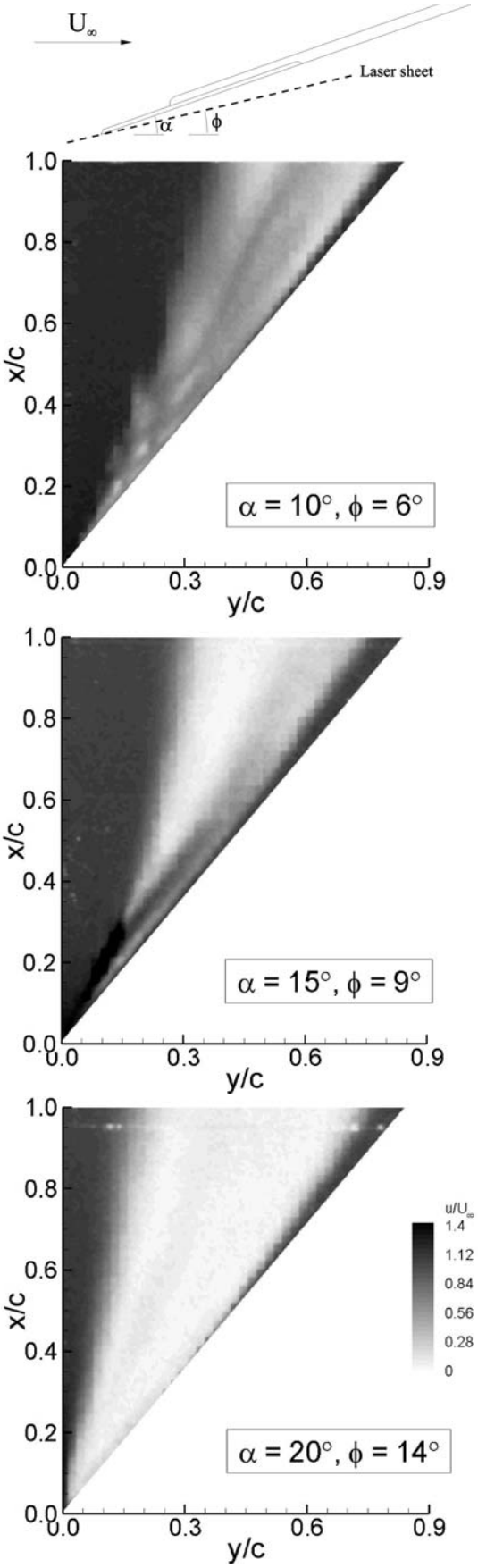


Figure 12. Magnitude of velocity in a plane through the vortex core[35].

https://doi.org/10.1017/S0001924000000269 Published online by Cambridge University Press

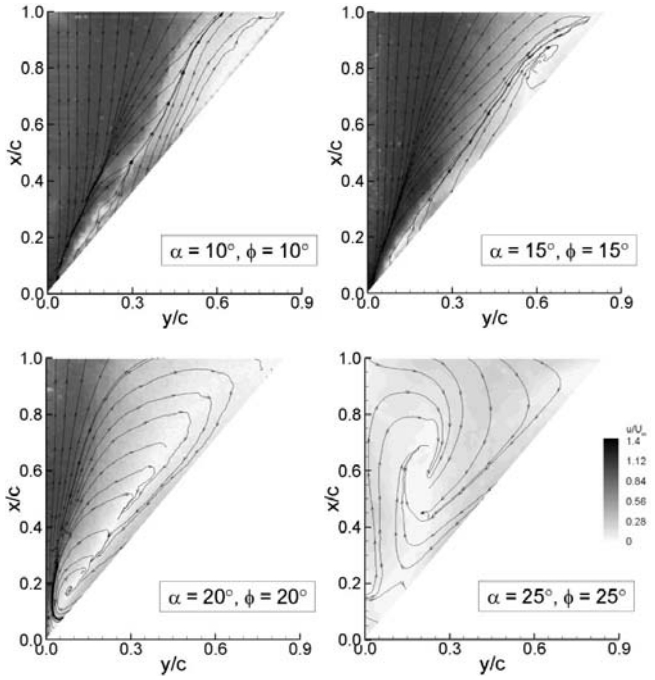


Figure 13. Magnitude of time-averaged velocity and streamline pattern near the wing surface[35].

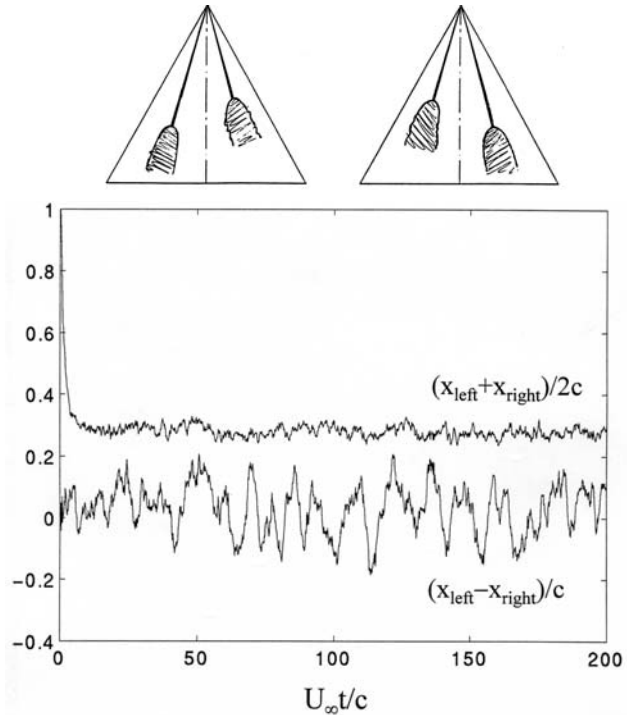


Figure 14. Time history of average and difference of breakdown locations showing antisymmetric oscillations[37]. The inset shows these oscillations schematically.

vortex breakdown is weak and difficult to identify, as there is no complete flow stagnation. At $\alpha = 15^{o}$, a clearly defined jet-like axial flow in the vortex core and a clear breakdown region are observed. Hence, there are some similarities to slender wings at relatively higher incidences, but the breakdown is not as abrupt as those observed over slender delta wings. The breakdown region is conical in shape, with an apparent inboard shift of the vortex axis after

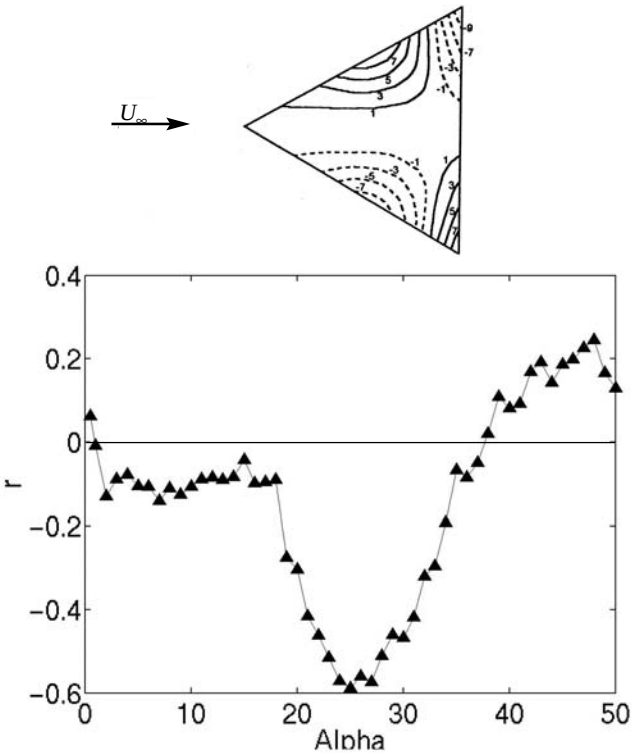


Figure 15. Variation of correlation coefficient between the left and right tip accelerations as a function of incidence[40].

breakdown. At $\alpha = 20^{o}$, the vortex structure has broken down, and a large conical region of stagnant flow is observed.

An indication of the near-surface flow pattern was obtained from the PIV measurements in a plane parallel to the wing surface[35]. The magnitude of the time-averaged velocity and the streamline pattern are shown in Fig. 13. The most important feature is that, for $\alpha = 20^{o}$, flow reattachment occurs even though there is no streamwise vortex flow at this incidence (see also Fig. 12). Hence, unlike slender delta wings, flow reattachment is possible at high incidences. Eventually, at the largest incidence $\alpha = 25^{o}$, the shear layer reattachment fails entirely, being replaced by a flow feature described in previous research[29] as a 'whorl'.

4.0 VORTEX INTERACTIONS

It was observed in several experiments that the vortex breakdown location over stationary slender delta wings is not steady and exhibits fluctuations along the axis of the vortices[36]. Subsequently it was discovered that these oscillations are in the form of an anti-symmetric motion of breakdown locations for left and right vortices[37]. Time history of average breakdown location $(x_{left} + x_{right})/2c$ and difference between the breakdown locations $(x_{left} - x_{right})/c$ are shown in Fig. 14 for $\alpha = 37^{o}$ and $\Lambda = 70^{o}$. The two breakdowns, which are almost mirror images, oscillate in an antisymmetric motion. The amplitude of these fluctuations can be a significant fraction of the chord length. It is also seen that oscillations of breakdown locations are quasi-periodic. The dominant frequency of the oscillations of breakdown location occurs at much lower frequencies than the frequency of the helical mode instability. In fact, it was shown by Menke *et al*[37] that the frequency of this organised motion is much smaller than the frequency of any other known instabilities. When compared with the frequency of other phenomena, the frequency range of oscillations of breakdown location for a stationary delta wing is much closer to the frequency range of typical aerodynamic

https://doi.org/10.1017/S0001924000000269 Published online by Cambridge University Press

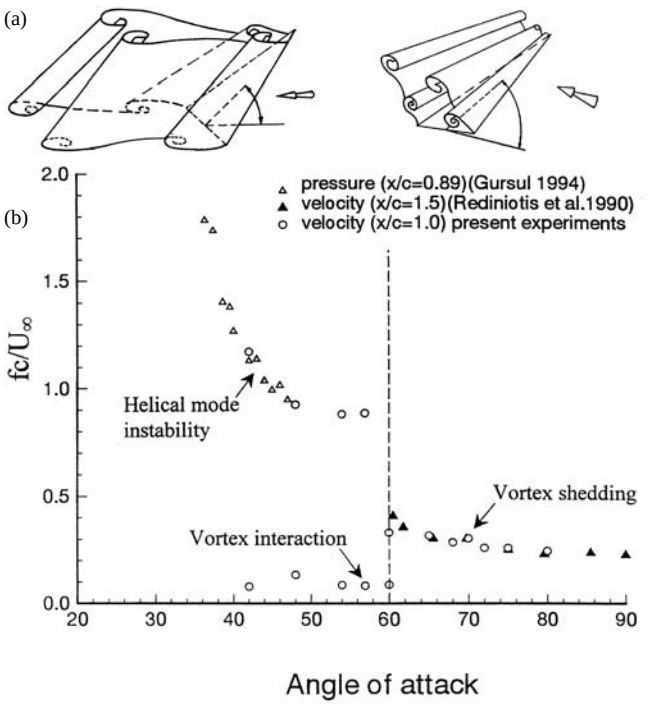


Figure 16. (a) Symmetric and antisymmetric modes of vortex shedding from delta wings[44]; (b) variation of dimensionless frequency for unsteady phenomena as a function of angle-of-attack[46].

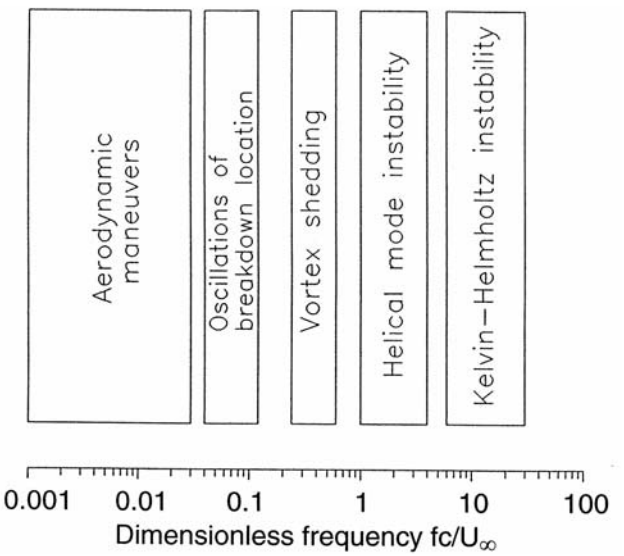


Figure 17. Spectrum of unsteady flow phenomena over delta wings as a function of dimensionless frequency[37].

manoeuvres (up to $fc/U_\infty \cong 0{\cdot}03$). The response of breakdown location and possible coupling between the wing motion and breakdown location in this frequency range is very important. It is noted that low Reynolds number observations of the vortex interactions in water-tunnel facilities were confirmed in the wind-tunnel experiments at much higher Reynolds numbers[38, 39].

In order to understand the mechanism leading to oscillations of the breakdown location, extensive experiments were conducted, and spectral analysis and other statistical concepts were used to quantify the unsteady behaviour of the vortex breakdown location obtained from flow visualisation[37]. It was found that oscillations become larger and more coherent as time-averaged breakdown locations get closer to each other when the angle-of-attack or sweep angle is increased. Although these kinds of vortex interactions are more of a concern for slender wings, evidence of such interactions at a relatively low sweep angle of $\Lambda = 60^\circ$ was recently reported[40]. Wing tip accelerations were mostly out-of-phase for a slightly flexible delta wing when vortex breakdown occurred on the wing. The variation of the correlation coefficient between the accelerations of left and right sides is shown in Fig. 15 as a function of angle-of-attack. For this sweep angle, vortex breakdown reaches apex around $\alpha \approx 34^\circ$, whereas the most negative correlation occurs around $\alpha \approx 25^\circ$, when vortex breakdown is close to apex.

The detailed mechanism that is responsible for this interaction is not clear. One possible mechanism is that the interaction is the result of a cross-flow instability. This is very similar to the well-known vortex asymmetry problem in forebody flows, except that the asymmetry for delta wing vortices is time-dependent while the time-averaged locations of vortex cores are symmetric. The oscillations of vortex cores could be imagined to arise from a loss of stability by the symmetric mean flow. It is possible that this interaction causes the location of breakdown to vary periodically in an antisymmetric motion. Periodic oscillations of vortex cores about mean symmetric positions have been observed in flow visualisation experiments for a circular cone[41]. This quasi-periodic phenomenon was observed visually near the onset angle-of-attack of asymmetry and over a certain range of Reynolds numbers. A recent theoretical study[42] revealed that vortices over a thin slender delta wing are stable to all disturbances of small amplitude based on the slender-body theory for an inviscid incompressible flow, but the vortices may become unstable with increasing wing thickness. A second possible mechanism is that the interaction is the result of a streamwise instability of breakdown regions, and vortex breakdown is a necessary part of the onset of the instability. Further studies are needed to clarify the physical mechanism of the interaction.

Vortex interactions over delta wings may become even more complex for manoeuvring aircraft. Recent research has shown that the dynamic response of breakdown location to small amplitude pitching oscillations of a delta wing may be very complex[43]. Depending on angle-of-attack and pitching frequency of the wing, breakdown locations may be phase-locked to the wing motion or may exhibit a mode competition between the symmetric and antisymmetric modes.

There is evidence of vortex interactions even after vortex breakdown reaches the apex and no streamwise vortex flow exists. Based on two-point velocity measurements in the wake of a delta wing, Rediniotis *et al*[44, 45] showed that vortex shedding occurs at large angles-of-attack. It was suggested that both symmetric and antisymmetric modes of shedding existed as sketched in the inset of Fig. 16, although the symmetric mode is more dominant for a slender wing. It was shown that this quasi-periodic phenomenon occurs over a wide range of angles-of-attack, without significant influence of the Reynolds number.

The transition from the helical mode instability (when vortex breakdown exists over the wing) to vortex shedding was studied in detail by Gursul and Xie[46]. Measurements of the streamwise velocity at the trailing-edge ($x/c = 1{\cdot}0$) and spectral analysis indicate that the helical mode instability of swirling flow disappears after vortex breakdown reaches the apex, and the dominant frequency of the vortex shedding appears in the spectra. The transition from the helical mode instability to the vortex shedding was found to be abrupt as indicated by a jump in the frequency parameter, and occurred at the angle-of-attack at which breakdown reached the apex (see Fig. 16). When the source of the quasi-periodic oscillations is the helical mode instability (for $\alpha < 60^\circ$), the measured frequencies at $x/c = 1{\cdot}0$ are much larger than those in the wake at $x/c = 1{\cdot}5$. This was explained by the significant changes in the wavelength of the helical mode instability in the streamwise direction in the near wake. On the other hand, when the source of the quasi-periodic oscillations is the vortex shedding (for $\alpha > 60^\circ$), the measured frequencies at $x/c = 1{\cdot}0$ and in the wake $x/c = 1{\cdot}5$ agree very well. This implies that the frequency of the vortex shedding is nearly constant in the near wake.

https://doi.org/10.1017/S0001924000000269 Published online by Cambridge University Press

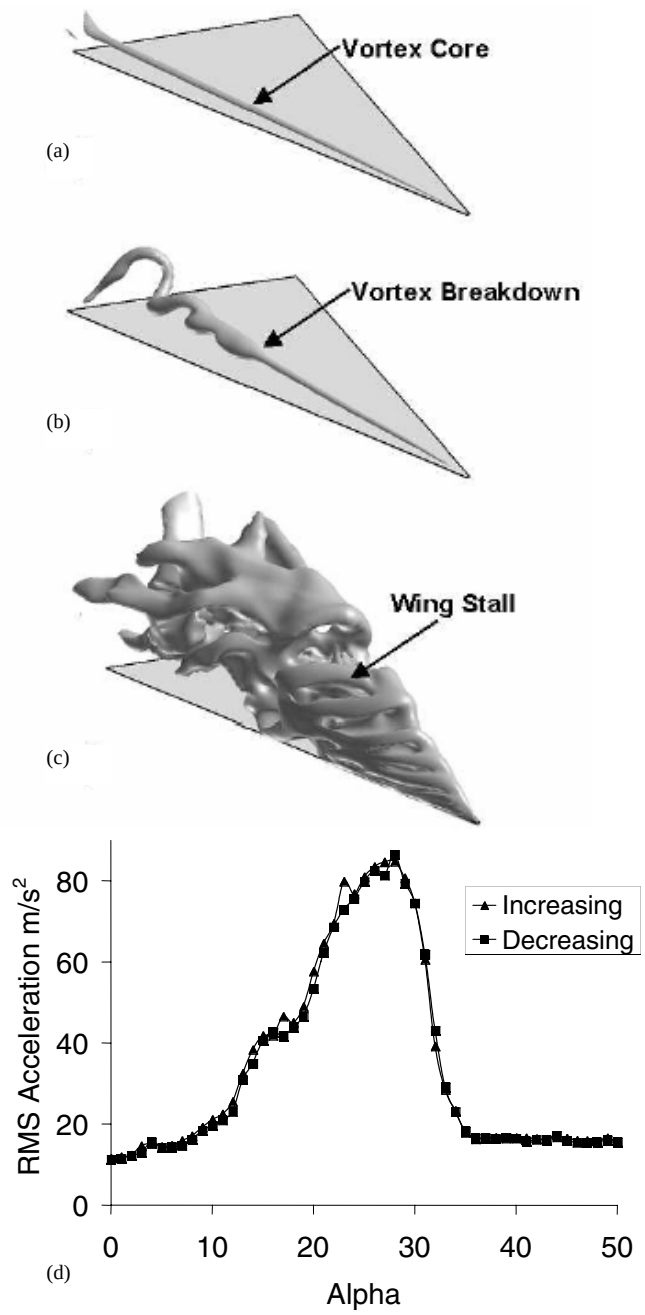


Figure 18. Types of flow regimes observed for a wing with $\Lambda = 60°$, (a) $\alpha = 5°$, (b) $\alpha = 15°$, (c) $\alpha = 40°$ (Ref. 48); (d) variation of rms tip acceleration as a function of incidence[40].

The spectrum of unsteady flow phenomena over slender delta wings as a function of dimensionless frequency is shown in Fig. 17. The frequency range of vortex shedding is also shown, although this phenomenon is distinctly different from other phenomena presented in the figure and is not observed until the vortex breakdown location reaches the apex.

5.0 BUFFETING

The above mentioned unsteady flow phenomena cause wing and fin buffeting over delta wings. The measurements of buffeting on a slender delta wing model were reported by Mabey[47]. When the vortex

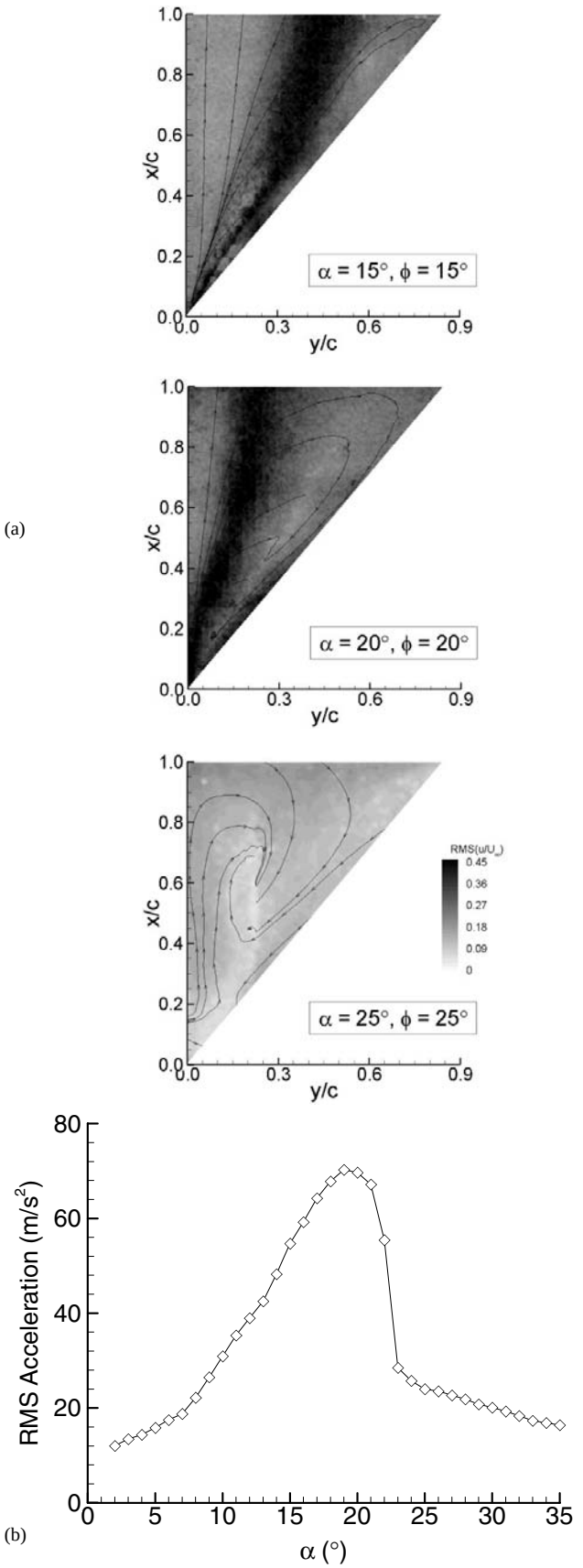


Figure 19. (a) Magnitude of rms velocity near the wing surface at different incidences for a wing with $\Lambda = 50°$; (b) variation of wing-tip rms acceleration with incidence[35].

https://doi.org/10.1017/S0001924000000269 Published online by Cambridge University Press

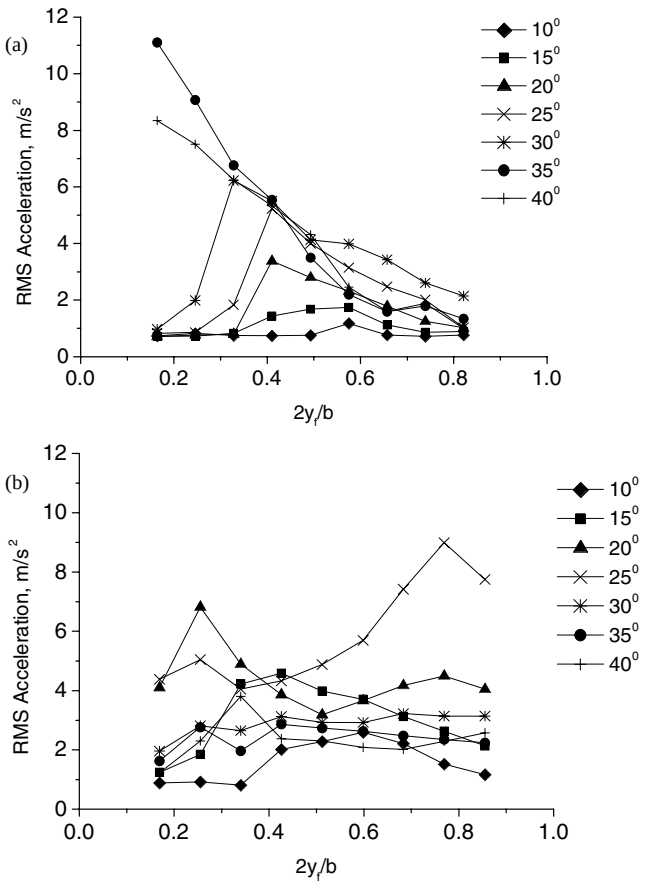


Figure 20. (a) Variation of rms acceleration as a function of fin location, $2y_f/b$, for $\Lambda = 75°$; (b) variation of rms acceleration as a function of fin location for $\Lambda = 50°$ (Ref. 57).

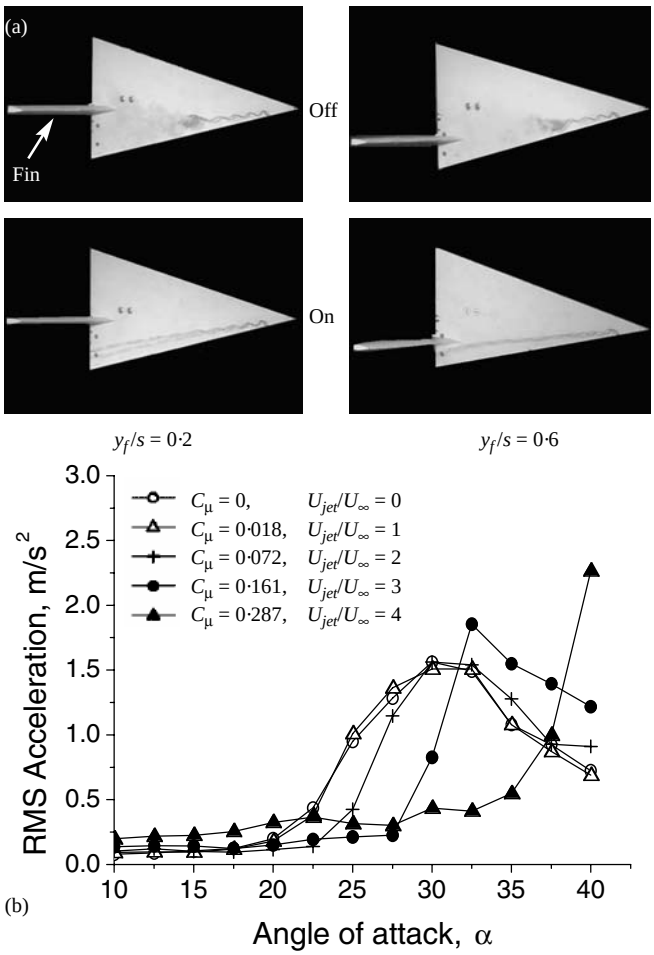


Figure 21. (a) Flow visualisation with and without jet blowing for two fin locations. The jet is located at the trailing edge with a deflection angle of $\beta = 30°$ and momentum coefficient of $C_\mu = 0{\cdot}708$; (b) variation of rms tip acceleration as a function of incidence for $y_f/s = 0{\cdot}4$ (Ref. 58).

breakdown location moved across the trailing edge, buffeting increased very rapidly. Also, sharply increased fluctuations in the normal force coefficient for delta wings were observed when vortex breakdown moved over the wing[29]. Hence the most important source of wing buffeting is the vortex breakdown phenomenon. Even for a $\Lambda = 60°$ wing, which may be regarded as the transitional case between the slender wing and nonslender wings, it was found that maximum rms (root-mean-square) buffeting[40] occurs when vortex breakdown is close to the apex of the wing (see Fig. 18). Also shown are the vortex regimes that were simulated computationally[48]. These Euler computations were used to simulate aeroelastic deformation of a slightly flexible delta wing due to unsteady vortical flows. Note that the rms acceleration drops very rapidly in the vortex shedding regime at higher angles-of-attack.

For nonslender wings, vortex breakdown may not be the dominant source of buffeting. For a $\Lambda = 50°$ delta wing, it was shown that when vortex breakdown exists at low incidences, the maximum velocity fluctuations near the wing surface are observed just underneath the vortex axis. Maximum buffeting occurs prior to the stall, after the vortex breakdown has reached the apex of the wing[35] (see Fig. 19). For this incidence $\alpha = 20°$, the largest velocity fluctuations near the wing surface are observed along the reattachment line. Hence, the shear layer reattachment, rather than the vortex breakdown phenomenon, is the most important source of increasing buffet in the pre-stall region as incidence is increased. With further increase in incidence, the shear layer reattachment becomes impossible, resulting in very low velocity fluctuations near the wing surface and a precipitous fall in the RMS wing tip acceleration.

Vortex breakdown is the major source of fin buffeting over slender delta wings. Distortion of incident vortex and interaction of vortex breakdown with fins have been investigated in detail[49, 50]. Measurements of unsteady surface pressure on fins generally showed that spectra had a dominant peak at high angle-of-attack due to the helical mode instability. Wolfe *et al*[51] reviewed a wide variety of investigations of both simplified fin-delta wing configurations and fins on actual model aircraft. They demonstrated that the shapes of the sur-

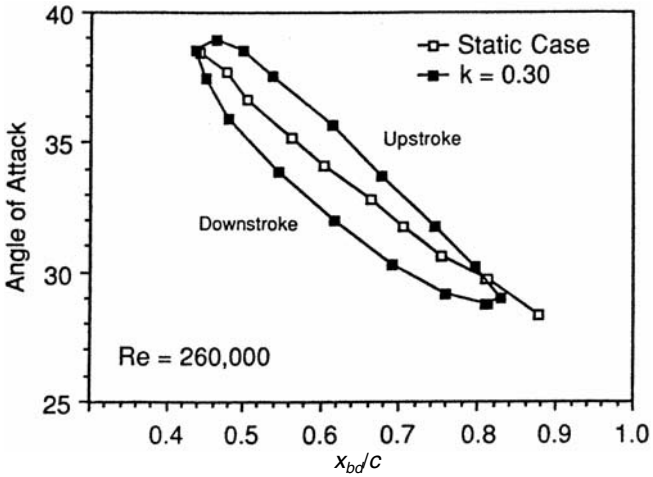


Figure 22. Chordwise location of vortex breakdown for a pitching delta wing[64].

https://doi.org/10.1017/S0001924000000269 Published online by Cambridge University Press

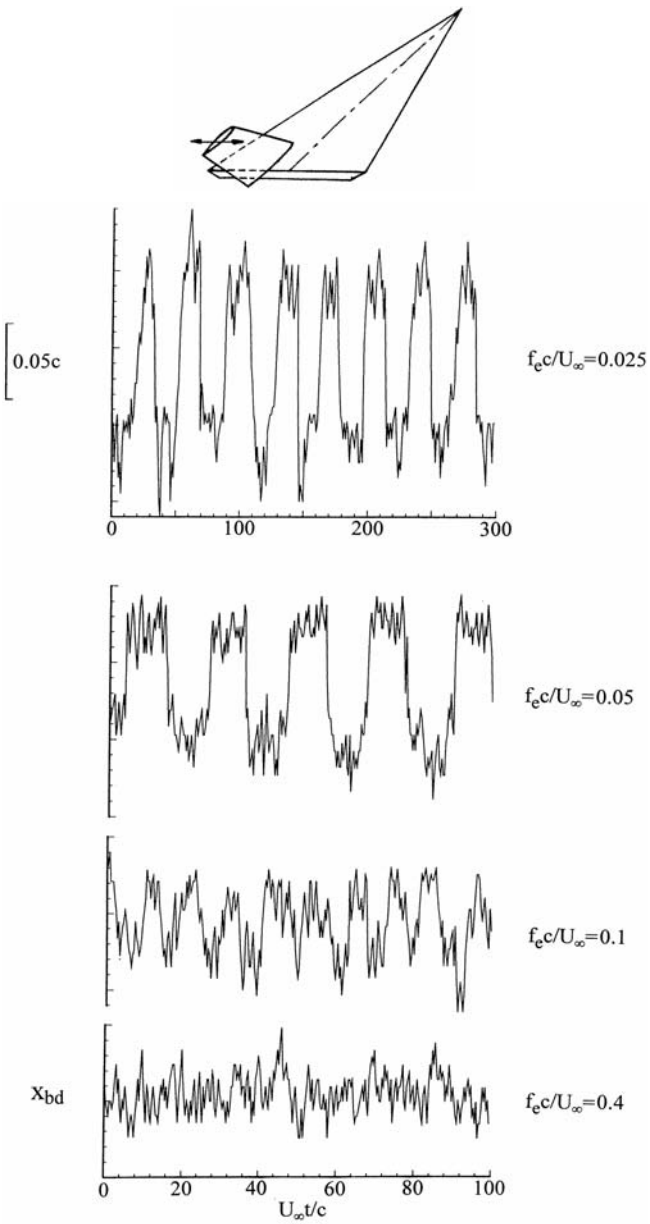


Figure 23. Time histories of breakdown location for different fin oscillation frequencies for a fin location of y_f/s = 0·8 (Ref. 55).

face pressure spectra are similar, and the dominant frequencies obey a simple scaling law over a wide range of Reynolds numbers (10^4 to 10^6). It was shown that the dimensionless frequency fx_{bd}/U_∞, where x_{bd} is the distance of breakdown location from the origin of the vortex, is roughly constant (with a value around unity). Wolfe *et al*[51] also show that dominant frequencies of surface pressure fluctuations on fins agree very well with those on the surface of delta wings[25] without a fin.

Although vortex breakdown is the major source of fin buffeting over slender delta wings, other unsteady phenomena can also contribute and even become the dominant source. Fluctuations of breakdown location[52], coupling between the unsteady flow separation over the fin surface and vortex breakdown[53, 54], aeroelastic effects[55] (fin surface deflections), and vortex shedding[56] may all contribute. Bean *et al*[56] demonstrated that fin buffeting is possible at very large angles-of-attack where a leading-edge vortex no longer exists.

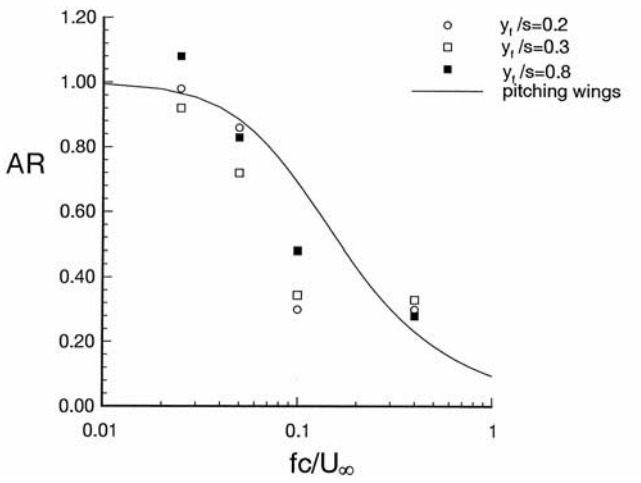


Figure 24. Variation of the amplitude ratio as a function of forcing frequency[55].

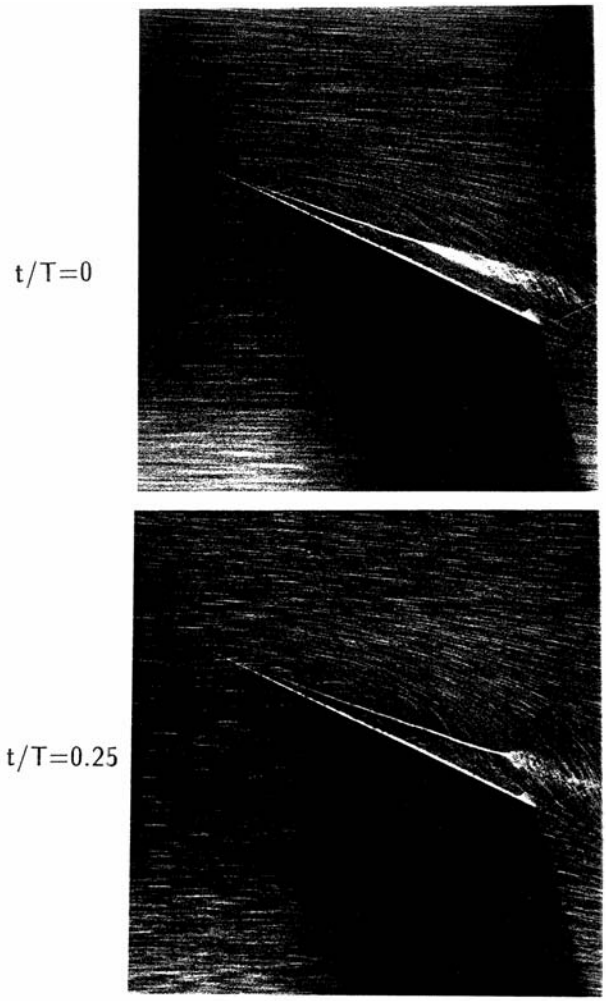


Figure 25. Flow visualisation of vortex breakdown for unsteady free stream, $U/U_\infty = 1 + R\mathrm{Cos}(\omega t)$, $\omega c/2U_\infty$ = 1·395, R = 0·70, α = 25°, Λ = 76° (Ref. 74).

The effect of wing sweep angle on the characteristics of fin buffeting over delta wings has recently been investigated[57]. For slender wings, there is a strong asymmetry with regard to the effect of fin location on the buffeting response, and the largest response occurs for the inboard fin locations (see Fig. 20(a)). For outboard fin

https://doi.org/10.1017/S0001924000000269 Published online by Cambridge University Press

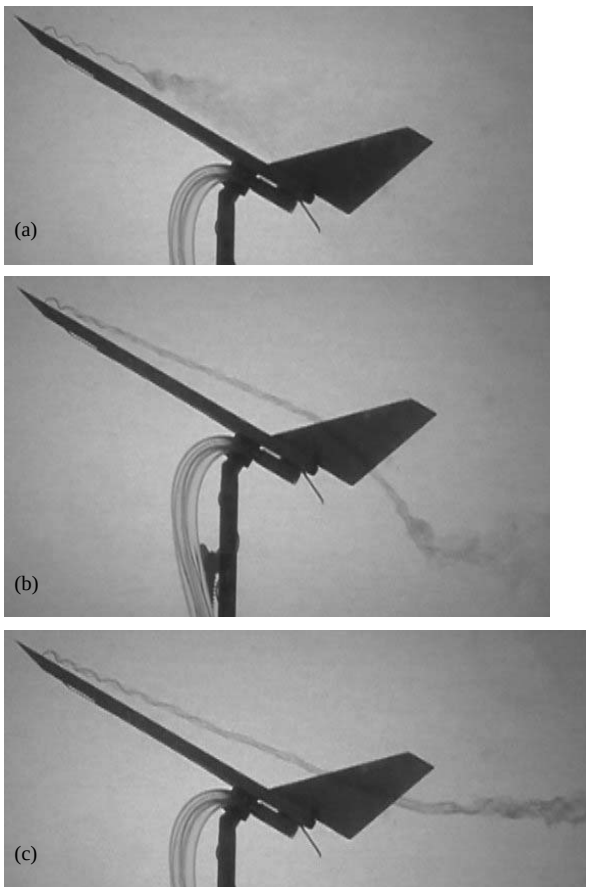


Figure 26. Flow visualisation of leading-edge vortex for (a) jet off, (b) just after jet is turned on, C_μ = 0·708, β = 30°, (c) just after the jet is turned off[58], α = 30°, Λ = 75°.

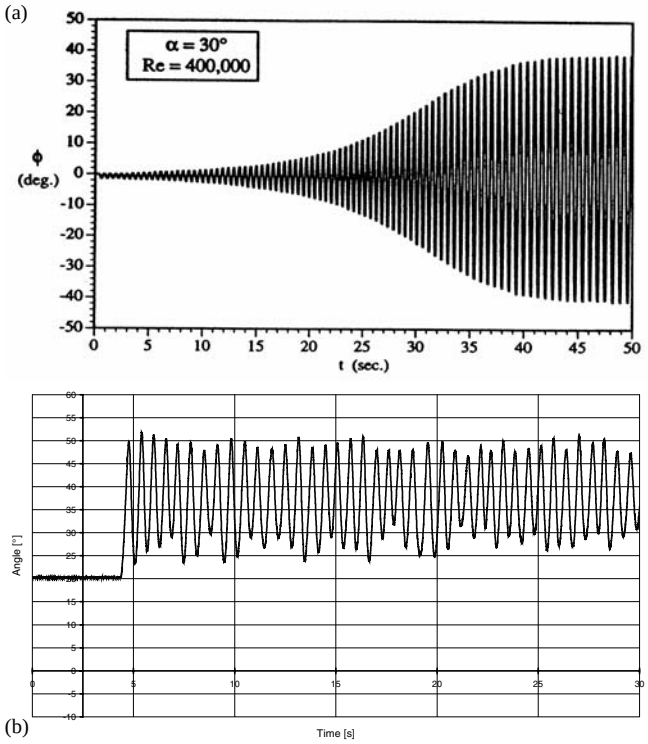


Figure 27. (a) Time history of wing rock for a slender delta wing, Λ = 80° (Ref. 75); (b) time history of wing rock for a nonslender wing with Λ = 50° (Ref. 76).

locations, the buffeting is small, even at high angles-of-attack when vortex breakdown is well upstream. For inboard fin locations, the largest fin vibrations were found for breakdown locations well upstream of the fin, and when the shear layer of the breakdown region impinges on the fin. The results show that single-fin buffeting may be as important as twin-fin buffeting. For a wing with low sweep angle, vortex shedding rather than vortex breakdown may become the responsible mechanism, and large buffeting excitation for outboard fin locations at a specific incidence is possible (see Fig. 20(b)). The impingement of separated shear layer on the fin can generate substantial buffeting in the post-stall regime for nonslender wings[57] at moderate incidences.

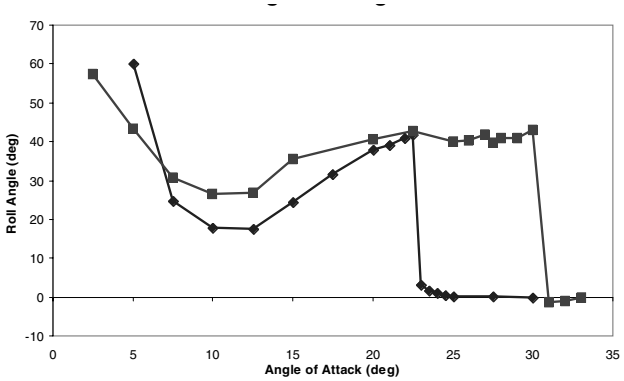
The presence of a fin generates an adverse pressure gradient, which is the dominant factor in determining the location of vortex breakdown and the magnitude of fin buffeting. When there is a jet at the trailing edge of the wing, the external pressure gradient can be altered. Figure 21(a) shows that vortex breakdown is induced as a result of the adverse pressure gradient imposed by the fin, but can be delayed into the wake when the jet is turned on. Even for the head-on collision of the leading-edge vortex with the fin, it was possible to eliminate the breakdown completely. This results in attenuation of buffeting of a flexible fin as shown in Fig. 21(b). In wind tunnel experiments, it was found that there was considerable delay (as much as 12º in incidence of the wing) of the onset of buffeting to higher angles-of-attack with increasing jet momentum. Jet-blowing at the trailing edge appears to be more effective at higher jet deflection angles.

6.0 DELTA WINGS IN UNSTEADY FLOWS

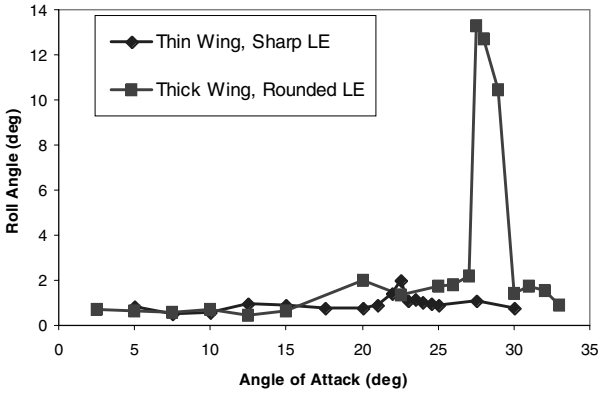
If a delta wing performs a manoeuvre or if free stream has unsteadiness, two effects may be observed: dynamic response of leading-edge vortex and vortex breakdown. Previous investigations on plunging[59, 60] and pitching[61] delta wings have shown that there is hysteresis and time lag in the development of the leading-edge vortex in a cross-flow plane. Similarly, the location of vortex breakdown has a time delay with respect to the quasi-steady case[62-65]. However, these two events have very different time scales. The time lag of vortex development is very small compared to the large time lag of breakdown location. An example of variation of location of vortex breakdown is shown in Fig. 22. The loops become wider with increasing frequency. It was also shown that the phase lag increases with increasing reduced frequency, without significant influence of the Reynolds number. This time lag, which is important for the stability and control of aircraft, has also been observed for other types of wing motion, such as plunging and rolling (see Greenwell and Wood[66] for a summary). The estimated values of the time constant for different types of motion are given by Srinivas *et al*[67] and Greenwell and Wood[66]. The normalised time constant $\tau U_\infty/c$, which is of the order of unity, depends on the type and amplitude of the motion, the breakdown location in the static case, and the sweep angle of the wing. For $\Lambda \geq 70^\circ$, the normalised time constant is around $\tau U_\infty/c$ = 1 to 2. For lower sweep angles, the time constant is larger. Recent investigations revealed similar time lags for a variety of unsteady motions, including pitching wings[62-65], oscillating leading-edge flaps[68], leading-edge extensions[69], wings undergoing oscillatory lateral motion[70], and an oscillating fin placed near the trailing-edge of a delta wing[55]. This suggests that the mechanism of time lag with respect to the quasi-steady case is universal regardless of the type of unsteady motion[71].

In the case of the oscillating fin, large oscillations of breakdown location[55] are possible. For excitation frequencies lower than a cut-

https://doi.org/10.1017/S0001924000000269 Published online by Cambridge University Press



(a) Time-averaged roll angle.



(b) Root-mean-square of roll angle.

Figure 28. Variation of (a) time-averaged roll angle, (b) root-mean-square of roll angle as a function of incidence for a thin wing with sharp leading edge and a thick wing with rounded leading edge[77].

off frequency (which is around $fc/U_\infty \approx 0{\cdot}40$), the response of vortex breakdown location is quasi-periodic, and the amplitude of the variations of breakdown location decreases with increasing frequency (see Fig. 23). For excitation frequencies higher than the cut-off frequency, vortex breakdown does not respond to fin oscillations. The amplitude ratio, which was defined as the ratio of the rms value of the fluctuations of breakdown location to its quasi-steady counterpart, is shown in Fig. 24 as a function of dimensionless frequency for different fin locations on the wing. It is seen that the amplitude ratio decreases with increasing frequency, and the amplitude attenuation is similar to that of a low-pass filter. It is also seen that the amplitude response is very similar for pitching delta wings and oscillating fins. In a recent investigation[72], it was found that vortex breakdown had a similar response to an oscillating body in the wake. A proposed mechanism based on the wave propagation characteristics of vortex flows was presented by Gursul and Xie[55].

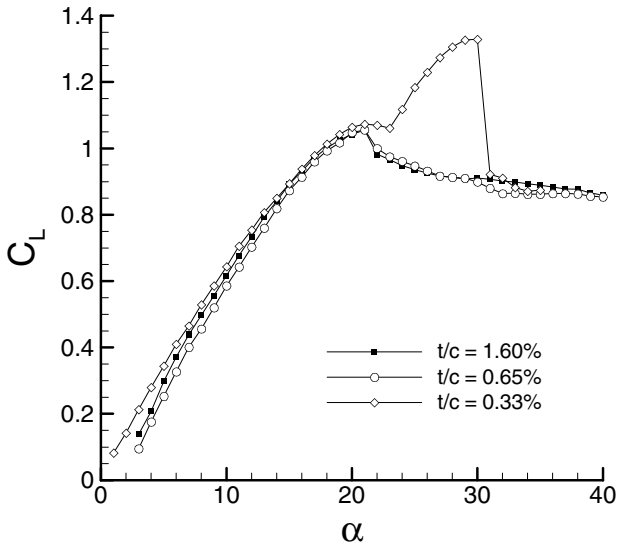
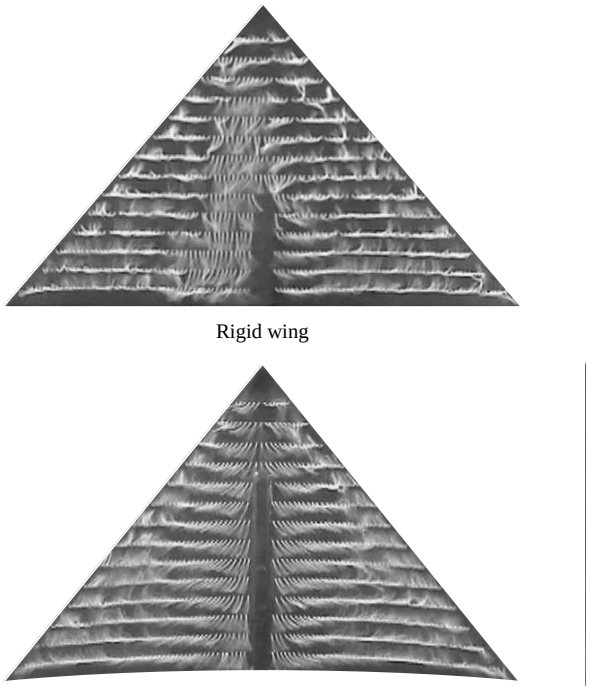


Figure 29. Variation of lift coefficient for various flexible delta wings, $\Lambda = 50°$ (Ref. 79).



Rigid wing

Flexible wing

Figure 30. Tuft visualisations showing surface flow patterns at $\alpha = 27°$, $\Lambda = 50°$.

Free stream unsteadiness may also affect vortex breakdown over a stationary delta wing[73]. If the vortex breakdown location is away from the trailing-edge and closer to the apex in steady free stream, the unsteadiness does not affect the burst position. Otherwise, the breakdown may appear suddenly at an upstream location, depending on the frequency[74] and amplitude as shown in Fig. 25. It was suggested that the time-dependent nature of the burst position is due to the relative variations in pressure gradient on the wing surface, which is expected to be more important near the trailing-edge. It is also noted that the shape and size of vortex breakdown region/wake may be very different in unsteady flows. For example, a highly elongated shape of breakdown at $t/T = 0$ is very unusual compared to the bubble type of breakdown at $t/T = 0{\cdot}25$.

The effect of thrust vectoring on wing vortex flows is another case where unsteady effects may be very strong. Figure 26 shows flow visualisation images[58] for (a) jet off, (b) just after jet is turned on, and (c) just after the jet is turned off. It is seen that the leading-edge vortex reacts rapidly for (b) and is drawn towards, and parallel to, the jet. When the jet is turned off, the wing vortex realigns itself to become almost parallel to the free stream. Vortex breakdown then slowly propagates upstream, and eventually reaches a steady-state location similar to that shown in Fig. 26(a). Hence time constants for the two cases are very different. Figure 26(c) also illustrates the hysteresis. The presence of large time-constants associated with this complex jet-vortex interaction is important for the dynamic aspects of thrust vectoring.

https://doi.org/10.1017/S0001924000000269 Published online by Cambridge University Press

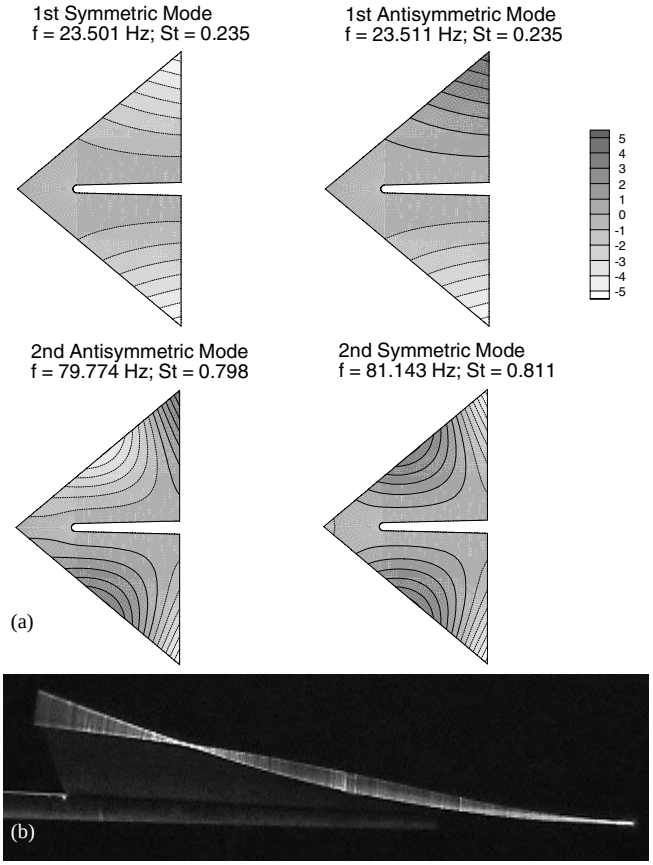


Figure 31. (a) Mode shapes predicted by finite element model; (b) deformation of the flexible wing (side view), $\Lambda = 50°$.

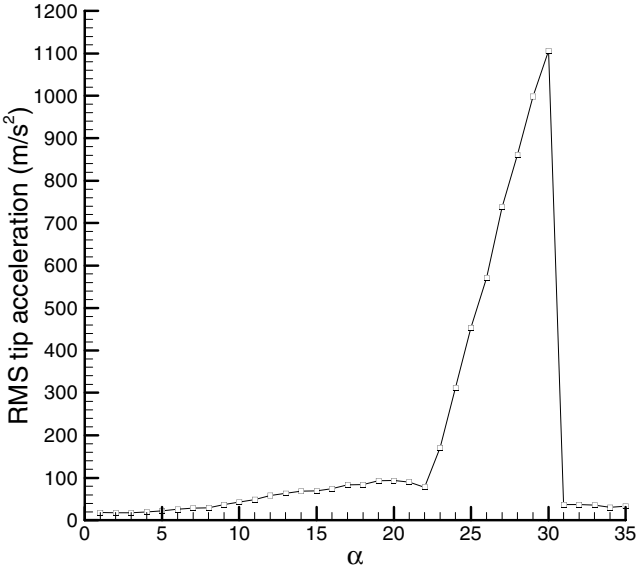


Figure 32. Variation of rms tip acceleration as a function of incidence.

7.0 FLOW–STRUCTURE INTERACTIONS

A well-known example of flow–structure interactions for delta wings is the occurrence of wing rock, which is a self-induced limit cycle roll oscillation for slender delta wings. An example of the time history of the roll angle is shown for a slender wing[75] with a sweep angle of $\Lambda = 80°$ in Fig. 27(a). The roll angle exhibits periodic oscillations around zero mean after a gradual build-up of the amplitude. Wing rock originates from the interaction of leading-edge vortices with wing, and is more typical for slender wings. Several aerodynamic phenomena[6] have been suggested as the mechanism(s) leading to the self induced oscillations, including vortex interactions, vortex asymmetries, breakdown, time lag of the position and strength of the vortices, and loss of roll damping.

Similar self-induced limit cycle oscillations are possible for non-slender delta wings, but their occurrence and flow physics are entirely different. An example of these unusual flow–structure interactions for a (free-to-roll) nonslender wing[76] with a sweep angle of $\Lambda = 50°$ is shown in Fig. 27(b). These oscillations are unusual because not only they are observed for a nonslender wing, but also the mean roll angle is nonzero. It is also interesting that these self-induced oscillations are observed over a small range of incidence. The mean roll angle and the amplitude of roll oscillations are shown as a function of incidence in Fig. 28. It is seen that the mean roll angle is nonzero for up to large incidences, which is a similar observation to the equilibrium positions of slender wings at nonzero roll angles. However, there are virtually no roll oscillations up to large incidences. In a critical and small range of incidence, the roll oscillations are large. With further increase in incidence, the mean roll angle becomes zero and the roll oscillations diminish. The self-induced roll oscillations are also observed for a sharp leading edge, but are much smaller than a rounded thick ($t/c = 0{\cdot}1$) wing[77]. This suggests that movement of the separation point at the leading edge is very important.

Flow–structure interactions for flexible delta wings are possible. The degree of coupling between the unsteady vortical flow and flexible wing is expected to be small for slightly flexible wings[40, 48]. However, for more flexible delta wings, the vortex acts like an aerodynamic spring and the coupling may result in limit-cycle-oscillations[78]. There might be substantial effects on the vortical flow and aerodynamic forces with increasing wing flexibility, as the oscillating leading edge is an unsteady source of vorticity. Recently, it was shown that substantial lift enhancement can be achieved on a flexible delta wing[79]. It is shown in Fig. 29 that passive lift enhancement over a flexible, low-sweep delta wing was achieved in the post-stall region, and increased the lift coefficient by up to 45%, and delayed stall by up to 9°. Figure 30 shows visualisations of the surface flow at $\alpha = 27°$ for the rigid and flexible wing. For the rigid wing, there is stalled flow, with large regions of reversed flow and large-scale unsteadiness. For the flexible wing, flow reattachment on the wing surface is evident.

Large time-averaged structural deflections and vibrations accompany this behaviour, along with a switching of dominant mode of vibration from the fundamental to the 2nd anti-symmetric mode (see Fig. 31(a) for the structural modes and Fig. 31(b) for the deformation of the wing in the region of lift enhancement). Figure 32 shows the variation of rms tip acceleration as a function of incidence. Comparison with Fig. 29 suggests that large vibrations occur in the region of lift enhancement. The existence of self-induced antisymmetric vibrations in this region is similar to the vortex interactions discussed in Section 4. There is evidence that while there is significant time-averaged deflection of the wing, particularly at high incidences, this does not contribute to the lift enhancement phenomenon[79]. On the other hand, the main mechanism for lift enhancement seems to be related to the excitation of the shear layer instabilities. The dominant frequency of structural vibration was around $St = 0{\cdot}75$, which compares well with the dominant frequencies of the shear layer instabilities. The self-induced vibrations of the wing energise the vortices shed into the shear layer and promote reattachment to the wing surface, resulting in delayed stall and increased lift. One of the remaining unresolved issues is the role of the antisymmetric vibrations and whether this is essential for lift enhancement.

https://doi.org/10.1017/S0001924000000269 Published online by Cambridge University Press

8.0 CONCLUSIONS

Recent developments in delta wing aerodynamics are reviewed. For slender delta wings, recent investigations shed more light on the unsteady aspects of shear-layer structure, vortex core and breakdown. The structure of the shear-layer instabilities, vortex wandering, correlation between the latter two, vortex breakdown and its helical mode instability are among the new understandings of unsteady flow phenomena over slender delta wings. For nonslender delta wings, substantial differences in the structure of the vortical flow and breakdown may exist. The dual vortex structure, existence of vortical flows and breakdown even at low incidences, reattachment of shear layer even when there is no streamwise vortex flow at higher incidences, and generally mild vortex breakdown are the main differences from slender wings. Vortex interactions (more generally interactions of flow from both leading edges of the wing) are generic to both slender and nonslender wings. Antisymmetric oscillations of vortex breakdown, symmetric and antisymmetric vortex shedding at high incidences, and self-induced antisymmetric vibrations of flexible wings are a few examples of such interactions. Various unsteady flow phenomena may cause buffeting of wings and fins, however vortex breakdown, vortex shedding, and shear layer reattachment (for nonslender wings) are the most dominant sources.

Dynamic response of vortex breakdown over delta wings in unsteady flows can be characterised by large time lags and hysteresis. Regardless of the type of unsteady motion, similar observations have been made, suggesting a universal mechanism. Unusual flow–structure interactions for nonslender wings in the form of self-excited roll oscillations (similar to wing rock for slender wings, but with entirely different flow physics) have been observed. Flexible wings can exhibit limit-cycle-oscillations as a result of vortex–structure interaction. Recent experiments have shown that substantial lift enhancement is possible on a flexible delta wing, accompanied by self-induced vibrations in an antisymmetric structural mode. This appears to be possible due to the excitation of shear layer and promotion of reattachment to the wing surface, resulting in delayed stall and increased lift.

ACKNOWLEDGEMENTS

Research programmes funded by the Air Force Office of Scientific Research, the European Office of Aerospace Research and Development, and the Engineering and Physical Sciences Research Council in the UK contributed to this review paper. The author is particularly indebted to his students and colleagues, especially Dr M. Visbal, Dr R. Gordnier and Dr G. Taylor for valuable discussions and comments on this paper.

REFERENCES

1. LEE, M. and HO, C-M. Lift force of delta wings, *Applied Mechanics Reviews*, 1990, **43**, (9), pp 209-221.
2. WERLE, H. Quelques resultants experimentaux sur les ailes en fleche, aux faibles vitesses, obtenus en tunnel hydrodynamique, *La Recherche Aeronautique*, September-October 1954, **41**.
3. DELERY, J.M. Aspects of vortex breakdown, *Progress in Aerospace Sciences*, 1994, **30**, pp 1-59.
4. ROCKWELL, D. Three-dimensional flow structure on delta wings at high angle-of-attack: experimental concepts and issues, AIAA Paper 93-0550, January 1993.
5. VISBAL, M.R. Computational and physical aspects of vortex breakdown on delta wings, AIAA Paper 95-0585, January 1995.
6. GURSUL, I. Review of unsteady vortex flows over slender delta wings, *J Aircr*, in print. See also AIAA-2003-3942, AIAA Applied Aerodynamics Conference, 23-26 June 2003, Orlando, FL.
7. GAD-EL-HAK, M. and BLACKWELDER, R.F. The discrete vortices from a delta wing, *AIAA J*, 1985, **23**, pp 961-962.
8. GAD-EL-HAK, M. and BLACKWELDER, R.F. Control of the discrete vortices from a delta wing, *AIAA J*, 1987, **25**, (8), pp 1042-1049.
9. CIPOLLA, K.M. and ROCKWELL, D. Small-scale vortical structures in crossflow plane of a rolling delta wing, *AIAA J*, 1998, **36**, (12), pp 2276-2278.
10. SHIH, C. and DING, Z. Trailing-edge jet control of leading-edge vortices of a delta wing, *AIAA J*, 1996, **34**, (7), pp 1447-1457.
11. GORDNIER, R. and VISBAL, M.R. Unsteady vortex structure over a delta wing, *J Aircr*, 1994, **31**, (1), pp 243-248.
12. RILEY, A.J. and LOWSON, M.V. Development of a three-dimensional free shear layer, *J Fluid Mechanics*, 1998, **369**, pp 49-89.
13. MITCHELL, A.M. and MOLTON, P. Vortical substructures in the shear layers forming leading-edge vortices, *AIAA J*, **40**, (8), 2002, pp 1689-1692.
14. VISBAL, M. and GORDNIER, R. On the structure of the shear layer emanating from a swept leading edge at angle-of-attack, AIAA Paper 2003-4016, June 2003.
15. MENKE, M. and GURSUL, I. Unsteady nature of leading edge vortices, *Physics of Fluids*, 1997, **9**, (10), pp 1-7.
16. BAKER, G.R., BARKER, S.J., BOFAH, K.K. and SAFFMAN, P.G. Laser anemometer measurements of trailing vortices in water, *J Fluid Mechanics*, 1974, **65**, part 2, pp 325-336.
17. DEVENPORT, W.J., RIFE, M.C, LIAPIS, S.I. and FOLLIN, G.J. The structure and development of a wing-tip vortex, *J Fluid Mechanics*, 1996, **312**, pp 67-106.
18. GURSUL, I. and XIE, W. Origin of vortex wandering over delta wings, *J Aircr*, 2000, **37**, (2), pp 348-350.
19. LAMBOURNE, N.C. and BRYER, D.W. The bursting of leading edge vortices: some observation and discussion of the phenomenon, Aeronautical Research Council, R&M 3282, 1962.
20. ESCUDIER, M. Vortex breakdown: observations and explanations, *Progress in Aerospace Sciences*, 1988, **25**, pp 189-229.
21. HALL, M.G. Vortex breakdown, *Annual Review of Fluid Mechanics*, 1972, **4**, pp 195-218.
22. LEIBOVICH, S. Vortex stability and breakdown: survey and extension, *AIAA J*, 1984, **22**, (9), pp 1192-1206.
23. GURSUL, I. Criteria for location of vortex breakdown over delta wings, *Aeronaut J*, May 1995, **99**, (985), pp 194-196.
24. GURSUL, I. and YANG, H. Vortex breakdown over a pitching delta wing, *J Fluids and Structures*, 1995, **9**, pp 571-583.
25. GURSUL, I. Unsteady flow phenomena over delta wings at high angle-of-attack, *AIAA J*, February 1994, **32**, (2), pp 225-231.
26. GARG, A.K. and LEIBOVICH, S. Spectral characteristics of vortex breakdown flowfields, *Physics of Fluids*, 1979, **22**, (11), pp 2053-2064.
27. TOWFIGHI, J. and ROCKWELL, D. instantaneous structure of vortex breakdown on a pitching delta wing, *AIAA J*, 1993, 31, (7), pp 1160-1162.
28. JUMPER, E.J., NELSON, R.C. and CHEUNG, K. A simple criterion for vortex breakdown, AIAA-93-0866, 31st Aerospace Sciences Meeting and Exhibit, 11-14 January 1993, Reno, NV.
29. EARNSHAW, P.B. and LAWFORD, J.A. Low-speed wind-tunnel experiments on a series of sharp-edged delta wings, ARC Reports and Memoranda No 3424, March 1964.
30. WENTZ, W.H. and KOHLMAN, D.L. Vortex breakdown on slender sharp-edged wings, *J Aircr*, March 1971, **8**, (3), pp 156-161.
31. OL, M.V. and GHARIB, M. leading-edge vortex structure of nonslender delta wings at low Reynolds number, *AIAA J*, January 2003, **41**, (1), pp 16-26.
32. GURSUL, I., TAYLOR, G. and WOODING, C. Vortex flows over fixed-wing micro air vehicles, AIAA 2002-0698, 40th AIAA Aerospace Sciences Meeting & Exhibit, 14-17 January 2002, Reno, NV.
33. TAYLOR, G.S., SCHNORBUS, T. and GURSUL, I. An Investigation of vortex flows over low sweep delta wings, AIAA-2003-4021, AIAA Fluid Dynamics Conference, 23-26 June 2003, Orlando, FL.
34. GORDNIER, R.E. and VISBAL, M.R. Higher-order compact difference scheme applied to the simulation of a low sweep delta wing flow, AIAA 2003-0620, 41st AIAA Aerospace Sciences Meeting and Exhibit, 6-9 January 2003, Reno, NV.
35. TAYLOR, G. and GURSUL, I. Unsteady vortex flows and buffeting of a low sweep delta wing, AIAA-2004-1066, 42nd Aeropsace Sciences Meeting and Exhibit, 3-8 January 2004, Reno, Nevada. See also, TAYLOR, G.S. and GURSUL, I. Buffeting flows over a low-sweep delta wing, *AIAA J*, in print.
36. GURSUL, I. and YANG, H. On fluctuations of vortex breakdown location, *Physics of Fluids*, **7**, (1), 1995, pp 229-231.
37. MENKE, M., YANG, H., and GURSUL, I. Experiments on the unsteady nature of vortex breakdown over delta wings, *Experiments in Fluids*, 1999, **27**, (3), pp 262-272.

https://doi.org/10.1017/S0001924000000269 Published online by Cambridge University Press

38. MITCHELL, A.M., BARBERIS, D. and DELERY, J. Oscillation of vortex breakdown location and its control by tangential blowing, AIAA Paper 98-2914, 1998.
39. LAMBERT, C. and GURSUL, I. Insensitivity of unsteady vortex interactions to Reynolds number, *AIAA J*, 2000, **38**, (5), pp 937-939.
40. GRAY, J.M., GURSUL, I., and BUTLER, R. Aeroelastic response of a flexible delta wing due to unsteady vortex flows, AIAA-2003-1106, 41st Aerospace Sciences Meeting and Exhibit, 6-9 January 2003, Reno, Nevada.
41. STAHL, W.H. and ASGHAR, A. Change of asymmetric vortex-flow pattern as function of Reynolds number and incidence behind circular cone, AIAA Paper 96-3389, 1996.
42. HUANG, M.K. and CHOW, C.Y. Stability of leading-edge vortex pair on a slender delta wing, *AIAA J*, 1996, **34**, (6), pp 1182-1187.
43. MENKE, M. and GURSUL, I. Nonlinear response of vortex breakdown over a pitching delta wing, *J Aircr*, 1999, **36**, (3), pp 496-500.
44. REDINIOTIS, O.K., STAPOUNTZIS, H. and TELIONIS, D.P. Vortex shedding over delta wings, *AIAA J*, 1990, **28**, (5), pp 944-946.
45. REDINIOTIS, O.K., STAPOUNTZIS, H. and TELIONIS, D.P. Periodic vortex shedding over delta wings, *AIAA J*, 1993, **31**, pp 1555-1562.
46. GURSUL, I. and XIE, W. Buffeting flows over delta wings, *AIAA J*, 1999, **37**, (1), pp 58-65.
47. MABEY, D.G. Beyond the buffet boundary, *Aeronaut J*, April 1973, **77**, pp 201-215.
48. GORDNIER, R.E. and VISBAL, M.R. Computation of the aeroelastic response of a flexible delta wing at high angles-of-attack, AIAA-2003-1728.
49. CANBAZOGLU, S., LIN, J.C., WOLFE, S. and ROCKWELL, D. Buffeting of fins: distortion of incident vortex, *AIAA J*, November 1995, **33**, (11), pp 2144-2150.
50. MAYORI, A. and ROCKWELL, D. Interaction of a streamwise vortex with a thin plate: a source of turbulent buffeting, *AIAA J*, October 1994, **32**, (10), pp 2022-2029.
51. WOLFE, S., CANBAZOGLU, S., LIN, J.C. and ROCKWELL, D. Buffeting of fins: an assessment of surface pressure loading, *AIAA J*, 1995, **33**, (11), pp 2232-2234.
52. WOLFE, S., LIN, J.C. and ROCKWELL, D. Buffeting at the leading-edge of a flat plate due to a streamwise vortex: flow structure and surface pressure loading, *J Fluids and Structures*, 1995, **9**, pp 359-370.
53. PATEL, M.H. and HANCOCK, G.J. Some experimental results of the effect of a streamwise vortex on a two-dimensional wing, *Aeronaut J*, April 1974, **78**, pp 151-155.
54. GORDNIER, R.E. and VISBAL, M.R. Numerical simulation of the impingment of a streamwise vortex on a plate, AIAA-97-1781, 28th AIAA Fluid Dynamics Conference, 29 June-2 July 1997, Snowmass Village, CO.
55. GURSUL, I. and XIE, W. Interaction of vortex breakdown with an oscillating fin, *AIAA J*, 2001, **39**, (3), pp 438-446.
56. BEAN, D.E., GREENWELL, D.I, and WOOD, N.J. Vortex control technique for the attenuation of fin buffet, *J Aircr*, 1993, **30**, (6), pp 847-853.
57. LAMBERT, C. and GURSUL, I. Characteristics of fin buffeting over delta wings, *J Fluids and Structures*, in print.
58. PHILLIPS, S., LAMBERT, C. and GURSUL, I. Effect of a trailing-edge jet on fin buffeting, *J Aircr*, 2003, **40**, (3), pp 590-599.
59. MALTBY, R.L., ENGLER, P.B. and KEATING, R.F.A. Some exploratory measurements of leading-edge vortex positions on a delta wing oscillating in heave, Aeronautical Research Council, R&M 3410, July 1963.
60. LAMBOURNE, N.C., BRYER, D.W. and MAYBREY, J.F.M. The behaviour of the leading-edge vortices over a delta wing following a sudden change of incidence, Aeronautical Research Council, R&M 3645, March 1969.
61. GAD-EL-HAK, M. and HO, C.M. The pitching delta wing, *AIAA J*, 1985, **23**, (11), pp 1660-1665.
62. ATTA, R. and ROCKWELL, D. Hysteresis of vortex development and breakdown on an oscillating delta wing, *AIAA J*, 1987, **25**, (11), pp 1512-1513.
63. ATTA, R. and ROCKWELL, D. Leading-edge vortices due to low Reynolds number flow past a pitching delta wing, *AIAA J*, June 1990, **28**, (6), pp 995-1004.
64. LEMAY, S.P., BATILL, S.M. and NELSON, R.C. Vortex dynamics on a pitching delta wing, *J Aircr*, February 1990, **27**, (2), pp 131-138.
65. VISBAL, M.R. Onset of vortex breakdown above a pitching delta wing, *AIAA J*, August 1994, **32**, (8), pp 1568-1575.
66. GREENWELL, D.I. and WOOD, N.J. Some observations on the dynamic response to wing motion of the vortex burst phenomenon, *Aeronaut J*, February 1994, **98**, (972), pp 49-59.
67. SRINIVAS, S., GURSUL, I. and BATTA, G. Active control of vortex breakdown over delta wings, AIAA 94-2215, 25th AIAA Fluid Dynamics Conference, 20-23 June 1994, Colorado Springs, CO.
68. DENG, Q. and GURSUL, I. Vortex breakdown over a delta wing with oscillating leading edge flaps, *Experiments in Fluids*, 1997, **23**, pp 347-352.
69. YANG, H. and GURSUL, I. Vortex breakdown over unsteady delta wings and its control, *AIAA J*, 1997, **35**, (3), pp 571-574.
70. TAYLOR, G. Support Interference in Oscillatory Dynamic Tunnel Testing, PhD Thesis, 2003, University of Bath, United Kingdom.
71. GURSUL, I. Proposed mechanism for time lag of vortex breakdown location in unsteady flows, *J Aircr*, 2000, **37**, (4), pp 733-736.
72. TAYLOR, G., GURSUL, I. and GREENWELL, D.I. An investigation of support interference in high angle-of-attack testing, *J Aircr*, 2003, **40**, (1), pp 143-152.
73. GURSUL, I. and HO, C-M. Vortex breakdown over delta wings in unsteady freestream, *AIAA J*, February 1994, **32**, (2), pp 433-436.
74. GURSUL, I. and HO, C-M. Vortex breakdown over delta wings in unsteady freestream, AIAA-93-0555, 31st Aerospace Sciences Meeting and Exhibit, 11-14 January 1993, Reno, NV.
75. ARENA, A.S. and NELSON, R.C. experimental investigation on limit cycle wing rock of slender wings, *J Aircr*, September-October 1994, **31**, (5), pp 1148-1155.
76. HÜSCHLER, S. Wing rock of nonslender delta wings, Research Project Report, University of Bath, June 2003.
77. MCCLAIN, A. Aerodynamics of Nonslender Delta Wings, MPhil Thesis, University of Bath, Department of Mechanical Engineering, March 2004.
78. GORDNIER, R. and MELVILLE, R. Physical mechanisms for limit-cycle oscillations of a cropped delta wings, AIAA Paper 99-3796, June 1999.
79. TAYLOR, G.S. and GURSUL, I. Lift enhancement over a flexible delta Wing, AIAA-2004-2618, AIAA Flow Control Conference, June 2004, Portland, Oregon.

https://doi.org/10.1017/S0001924000000269 Published online by Cambridge University Press